

Manuscript Number: BBABIO-08-237R1

Title: Flavodoxin: a compromise between efficiency and versatility in the electron transfer from Photosystem I to Ferredoxin-NADP+ reductase

Article Type: Regular Paper

Keywords: Ferredoxin-NADPP+P reductase; Flavodoxin; protein-protein interaction; electron transfer; Photosystem I; transient interactions.

Corresponding Author: Dr. Milagros Medina, Biochemistry

Corresponding Author's Institution: Universidad de Zaragoza

First Author: Guillermina Goñi

Order of Authors: Guillermina Goñi; Beatriz Herguedas, Biochemistry; Manuel Hervás; José R Peregrina; Miguel A De la Rosa; Carlos Gómez-Moreno; José A Navarro; Juan A Hermoso; Marta Martínez-Júlvez; Milagros Medina, Biochemistry

Abstract: Under iron-deficient conditions Flavodoxin (Fld) replaces Ferredoxin in *Anabaena* as electron carrier from Photosystem I (PSI) to Ferredoxin-NADP+ reductase (FNR). Several residues modulate the Fld interaction with FNR and PSI, but no one appears as specifically critical for efficient ET. Fld shows a strong dipole moment, with its negative end directed towards the flavin ring. The role of this dipole moment in the processes of interaction and ET with positively charged surfaces exhibited by PSI and FNR has been analysed by introducing single and multiple charge reversal mutations on the Fld surface. Our data confirm that in this system interactions do not rely on a precise complementary surface of the reacting molecules. In fact, they indicate that the initial orientation driven by the alignment of dipole moment of the Fld molecule with that of the partner contributes to the formation of a bunch of alternative binding modes competent for the efficient ET

reaction. Additionally, the fact that Fld uses different interaction surfaces to dock to PSI and to FNR is confirmed.

Suggested Reviewers:

Response to Reviewers: Dear Sirs, this new version of the manuscript has been prepared having into account reviewers' comments (see below) and editorial suggestions.

Answers to reviewers' comments:

Reviewer 1

- The E61K Fld midpoint potential has been measured as required by the reviewer and it is now included in the ms. The data confirms "E61 is a major determinant for the observed changes".

- Part of the functional electron transfer characterization has been done involving the transition between Fldox and Fldsq, because experimental measurements are more reliable in these systems and also because they have previously been shown as a good model in the analysis of the systems where Fld is involved. These results consist mainly in those involving ET from PSI to Fld. The following sentence has been introduced in the results section to explain this fact: Reduction of Anabaena FldBoxB to the semiquinone state by PSIBrdB using laser-flash absorption spectroscopy has demonstrated to be a useful model to analyse the interaction forces and ET parameters involved in the physiological reaction. In addition, and although the Fldsq/Fldhq couple is with no doubt involved in shuttling electrons between PSI and FNR, a physiological role for the Fldox/Fldsq couple can not be precluded.

Additionally, when measuring processes between FNR and Fld, we indicate now which one corresponds to the main physiological function of Fld in the Photosynthetic chain.

Minor points and spelling errors:

- We have reduced the used of the verb "to result".
- Keywords: spelling error for Ferredoxin-NADP+ reductase. Corrected
- Minor points indicated by the reviewer have been corrected
- "Synechochoccus" has been corrected to "Synechococcus". Mention to the change of the name "Synechococcus elongatus" to "Thermosynechococcus elongatus" is done.
- In former Figure 2, now Figure 1: Potentials are given versus NHE, as in Table 1.

Reviewer 2:

As suggested by the reviewer the manuscript has been considerably shortened. We have also tried to make it less verbose.

Speculative considerations have been removed, as well as the section about di-flavin reductases in the discussion. Some of the aspects of these proteins are now just mentioned within the general discussion of Flds.

We have tried to avoid detailed descriptions of what is shown in tables.

Former Figure 1 has been moved to Supplementary Material.

Parts of former figures 6 and 7 have been now condensed in Figure 5. The rest of the information has been move to the Supplementary Material.

The abstract sentence: "Our data confirm that in this system interactions do not rely on a precise complementary surface of the reacting molecules, but rather on the initial orientation between the reacting molecules provided by the strong electrostatic component of the Fld molecule" has been rephrased as suggested.

Reviewer 3:

1. We agree with the reviewer that we refer mainly to our work in the introduction. However, this is the only system in which an exhaustive study has been done in a photosynthetic electron transfer chain involving Fld instead of Fd. There are no equivalent data from other authors. Nevertheless, as suggested by the reviewer we have removed references to our work not required in general aspects. More general references have been used when possible and reference Tiede, D.M., et al., (1993) Biochemistry 32, 4515-4531 has been included. Additionally, the manuscript mentions now the possibility of a different explanation of the observed saturation profile of the concentration dependence of rate constants, as indicated by the referee.

2. The reviewer is right, there was a mistake in the chlorophyll/P700 ratio in PS I samples. The samples used had a ratio 104/1. This is now indicated in the ms.

3. The reviewer was right about the sentence "ET reactions might not have as much specific requirements as other protein-protein interactions." It has been corrected in the manuscript.

Flavodoxin: a compromise between efficiency and versatility in the electron transfer from Photosystem I to Ferredoxin-NADP⁺ reductase

Guillermina Goñi^a, Beatriz Herguedas^a, Manuel Hervás^b, José R. Peregrina^a, Miguel A. De la Rosa^b, Carlos Gómez-Moreno^a, José A. Navarro^b, Juan A. Hermoso^c, Marta Martínez-Júlvez^a and Milagros Medina^{a,*}

^a Departamento de Bioquímica y Biología Molecular y Celular, Facultad de Ciencias and Instituto de Biocomputación y Física de Sistemas Complejos (BIFI), Universidad de Zaragoza, Zaragoza, Spain.

^b Instituto de Bioquímica Vegetal y Fotosíntesis, Universidad de Sevilla-CSIC, Sevilla, Spain.

^c Grupo de Cristalografía Molecular y Biología Estructural, Instituto Química-Física Rocasolano, Consejo Superior de Investigaciones Científicas, Serrano 119, 28006 Madrid, Spain.

*Correspondence to: Dr. Milagros Medina, Departamento de Bioquímica y Biología Molecular y Celular, Facultad de Ciencias, Universidad de Zaragoza, 50009-Zaragoza, Spain. Phone: +34 976762476. Fax: +34 976762123. E-mail: mmedina@unizar.es

Running title: Flavodoxin residues in electron transfer from PSI to FNR.

Key words: Ferredoxin-NADP⁺ reductase, Flavodoxin, protein-protein interaction, electron transfer, Photosystem I, transient interactions.

Abstract

Under iron-deficient conditions Flavodoxin (Fld) replaces Ferredoxin in *Anabaena* as electron carrier from Photosystem I (PSI) to Ferredoxin-NADP⁺ reductase (FNR). Several residues modulate the Fld interaction with FNR and PSI, but no one appears as specifically critical for efficient ET. Fld shows a strong dipole moment, with its negative end directed towards the flavin ring. The role of this dipole moment in the processes of interaction and ET with positively charged surfaces exhibited by PSI and FNR has been analysed by introducing single and multiple charge reversal mutations on the Fld surface. Our data confirm that in this system interactions do not rely on a precise complementary surface of the reacting molecules. In fact, they indicate that the initial orientation driven by the alignment of dipole moment of the Fld molecule with that of the partner contributes to the formation of a bunch of alternative binding modes competent for the efficient ET reaction. Additionally, the fact that Fld uses different interaction surfaces to dock to PSI and to FNR is confirmed.

Introduction

Ferredoxin NADP⁺ reductase (FNR) catalyses the electron transfer (ET) from Photosystem I (PSI) to NADP⁺. In plants, electrons are transferred from PSI to FNR by Ferredoxin (Fd), but in most cyanobacteria and some algae, under iron deprivation, Flavodoxin (Fld) can substitute for Fd. Fd and Fld are different in size, sequence, folding and cofactors ([2Fe-2S] for Fd and FMN for Fld). However, both can function in the midpoint potential range ~400 mV [1] and, alignment on the basis of their electrostatic potentials indicates overlapping of their strong negative potentials around their redox centres [2]. The surfaces of PSI and FNR where Fd and Fld bind contain mainly positive patches (Figure SP1), suggesting that electrostatic forces will contribute to the complex formation step preceding ET [3-5].

In cyanobacteria PSI assembles as a trimer, each monomer containing 12 proteins and more than 100 cofactors [6]. Electrons flow from the P700 reaction centre through a series of carriers to reach the terminal [4Fe-4S] clusters, F_X, F_A and F_B. The PsaC, PsaD and PsaE subunits contribute to the positively charged solvent accessible stromal site of PSI (Figure SP1A). The PsaC subunit binds F_A and F_B and cannot be deleted without loss of PSI activity; PsaD is important for electrostatic steering of Fd and Fld; and PsaE has been implicated in controlling lifetime and stabilisation of the PSI:Fd complex, in cyclic ET and/or in a ternary complex with FNR [5, 7]. K35 from PsaC on the *Chlamydomonas reinhardtii* PSI [8], as well as K106 from PsaD [9-11] and R39 on PsaE in *Synechocystis* [12], play key roles in binding of the protein acceptor. The nature of several *Anabaena* Fld side chains has been shown to contribute to the formation of a transient PSI:Fld complex. However, replacements had minor effects on the ET process itself, and for some mutants mechanisms involving no-transient complex formation were as efficient as the WT one [4, 13-15]. In *Anabaena* FNR, the surface

around the FAD group presents patches of positively charged residues (Figure SP1B). R16, K72, R264 and especially K75 are required as positively charged, while L76 and L78 must be hydrophobic, for the efficient interaction with both Fd and Fld [1, 16-18]. Key counterpart residues to those were found on the Fd surface, namely F65 and E94 [16, 17]. However, individual replacements of residues on the Fld surface indicated that they were not involved in crucial specific interactions with FNR [18-20].

Therefore, the interaction of Fld with its partners appears to be less specific than that of Fd. This is also suggested by docking models showing that Fld could orientate in different ways on the FNR surface without significantly altering the distance between the methyl groups of FAD and FMN and, keeping the molecular dipoles on FNR and Fld nearly collinear [21]. The parameters that regulate the Fld movement between its docking site on PSI and that on FNR during Fld-dependent photosynthetic ET are further studied in this work. Residues, T12, E16, E20, E61, E67, D126 and D144 have been replaced with positively charged or neutral side chains. The cooperative action of these residues has been analysed in the E16K/E61K, E16K/D126K, E16K/E20K/D126K and E16K/E61K/D126K/D150K Flds. Finally, K2 and K3, residues producing one of the few accumulations of positive potential on the Fld surface, were simultaneously replaced by producing the K2A/K3A and K2E/K3E Flds. The effect of these mutations on the association and ET processes of Fld with PSI and FNR are discussed on the bases of the changes produced in the surface electrostatic potential and the dipole moment magnitude and orientation, as well as on the structural bases that regulate midpoint-reduction parameters.

MATERIALS AND METHODS

Site directed mutagenesis, protein expression and purification.

Mutations at K2, K3, T12, E16, E20, E61, D126 and D150 were introduced into the pTrc99a plasmid encoding the *Anabaena* Fld gene by PCR-based site-directed mutagenesis using the Stratagene QuikChange Kit (see supplementary material, SP) [14]. Multiple mutations were sequentially introduced after several rounds of mutagenesis. Mutations were verified by DNA sequence analysis and MALDI-TOF mass spectrometry. WT and mutated pTrc99a-Fld plasmids were overexpressed in *Escherichia coli* TG1 strain. Recombinant *Anabaena* PCC 7119 WT FNR, WT Fld and mutated Flds were purified from LB cultures of IPTG-induced *E. coli* [14]. UV/Vis spectra and SDS-PAGE were used as purity criteria. *Anabaena* PCC 7119 PSI particles were obtained as described [22]. The P700 content in PSI samples was calculated from the photoinduced absorbance changes at 820 nm, $\epsilon = 6.5 \text{ mM}^{-1} \text{ cm}^{-1}$. Chlorophyll concentration was determined according to Arnon [23]. The chlorophyll/P700 ratio of the PSI preparation was 104/1. The same batches of PSI and proteins were used throughout this study.

Spectral analyses.

UV-visible spectral measurements were carried out on a Kontron Uvikon 942, an Agilent HP 8453 or a Varian Cary 100 Bio spectrophotometer. Measurements were carried out at 25°C in 50 mM Tris/HCl, pH 8.0. Extinction coefficients of Fld_{ox}s were determined as described [24]. Other extinction coefficients were; $\epsilon_{\text{FNR}_{\text{ox}},458\text{nm}} = 9.4 \text{ mM}^{-1} \text{ cm}^{-1}$, $\epsilon_{\text{Cyt}_{\text{ox}},550\text{nm}} = 8.4 \text{ mM}^{-1} \text{ cm}^{-1}$ and $\epsilon_{\text{Cyt}_{\text{rd}},550\text{nm}} = 29.5 \text{ mM}^{-1} \text{ cm}^{-1}$. Stepwise anaerobic photoreduction of Flds was carried out in the presence of 2 μM 5-deazariboflavin (5-dRf) and 3 mM EDTA [13] and used to determine the percentage of maximum semiquinone stabilised and its extinction coefficient (see SP). Dissociation constants (K_d), extinction coefficient changes ($\Delta\epsilon$) and free energy (ΔG°) for complex formation between WT FNR_{ox} and the Fld_{ox} variants were obtained by difference

absorption spectroscopy [14]. Fitting of the experimental data to the theoretical equation for a 1:1 complex allowed the calculation of K_d and $\Delta\epsilon$. Errors in the determined K_d and $\Delta\epsilon$ values were $\pm 15\%$, and $\pm 10\%$ for ΔG° . The FNR NADPH-cytochrome *c* reductase activity was assayed by using the Fld mutants as electron carrier from FNR to cytochrome *c* (Cyt*c*) (Sigma) [25]. Errors in the estimated K_m and k_{cat} values were $\pm 15\%$ and $\pm 10\%$, respectively.

Oxido-reduction potential determinations.

Midpoint reduction potentials were determined in a protein solution combining potentiometric measurements of the oxido-reduction potential with optical measurements [13, 15]. Experiments were carried out by photoreduction of $\sim 40\text{ }\mu\text{M}$ Fld in the presence of $2\text{ }\mu\text{M}$ 5-dRf, 3 mM EDTA and $\sim 2\text{ }\mu\text{M}$ of each mediator dye at $25\text{ }^\circ\text{C}$ in 50 mM Tris/HCl pH 8.0, in an anaerobic cuvette, using a gold electrode and a saturated calomel electrode (details in supplementary material). Errors in the $E_{ox/sq}$ and $E_{sq/hq}$ were estimated to be $\pm 5\text{ mV}$.

Fast kinetic stopped-flow measurements.

Stopped-flow measurements were carried out under anaerobic conditions using an Applied Photophysics SX17.MV spectrophotometer [14]. Reduced samples of FNR and Fld were prepared by photoreduction. Reactions were followed after mixing the proteins at a $\sim 1:1$ molar ratio with a final concentration of $\sim 10\text{ }\mu\text{M}$ for each protein, in 50 mM Tris/HCl pH 8.0 at $10\text{ }^\circ\text{C}$. Processes between FNR and Fld were followed at 600 nm and, those between Fld_{hq} and $\text{Cyt}_{c_{ox}}$ at 550 nm . The apparent observed rate constants (k_{ap}) were calculated by fitting the data to mono- or bi-exponential processes. Each kinetic trace was the average of 20-30 measurements. Each experiment was repeated three times. Maximal errors in the determined k_{ap} values were $\pm 15\%$.

Fast kinetic laser-flash absorption spectroscopy measurements.

ET processes between PSI and Fld were followed at 580 nm by laser-flash absorption spectroscopy [14]. The standard reaction mixture contained in 1 ml, 20 mM Tricine/KOH, pH 7.5, 0.03 % β -dodecyl maltoside, an amount of PSI-enriched particles equivalent to 50 μ g of chlorophyll ml⁻¹, 0.05 μ M phenazine methosulfate, 2 mM MgCl₂, 2 mM sodium ascorbate, and Fld at the indicated concentration. The experiments at increasing MgCl₂ concentrations were carried out with a final Fld concentration of 20 μ M. Each kinetic trace was the average of 40-50 measurements, with 30 s intervals between flashes. Observed rate constants (k_{obs}) were obtained from 2-3 different experiments and analyses were carried out according to the two-step reaction mechanism [14]. Error in the determination was < 20 %.

Crystal growth, data collection, and structure refinement.

Crystals of K2A/K3A, E16K/E61K and E16K/E61K/D126K/D150K Flds were obtained by the hanging drop method: for K2A/K3A and E16K/E61K Fld, 1.5-2 μ l of a 5 mg/ml protein solution in Tris/HCl pH 8.0 were mixed with 1 μ l of reservoir solution consisting of 32 % PEG 4000, 0.2-0.3 M MgCl₂ and 0.1 M Tris/HCl pH 8.5; for E16K/E61K/D126K/D150K Fld, 1 μ l of a 5 mg/ml protein solution buffered with 0.1 M Tris/HCl pH 8.0 was mixed with 1 μ l of reservoir solution consisting of 22 % PEG 8000 and 0.2 M CaCl₂ buffered with 0.1 M MES, pH 6.5. The X-ray data set of the K2A/K3A Fld crystal was collected at the BM16 beamline of the ESRF on an ADSC Quantum210 detector with a wavelength of 0.97918 \AA . Data for E16K/E61K and E16K/E61K/D126K/D150K Flds were collected with a Kappa 2000 CCD detector using a graphite monochromated CuK α radiation generated by a Bruker-Nonius rotating anode. Data collection and refinement statistics are shown in Table SP1. The V_m are 1.95, 1.99 and 1.96 $\text{\AA}^3/\text{Da}$ and over 36.8 %, 38.2 % and 37.4 % solvent contents for K2A/K3A, E16K/E61K and E16K/E61K/D126K/D150K Flds, respectively. Data were

processed, scaled and reduced with HKL2000 [26]. The mutant structures were solved by molecular replacement, using the program MOLREP [27] and the native Fld_{ox} structure (PDB code 1flv). Refinement was made using the programs CNS [28] and REFMAC [29] and manual model building by the graphics program “O” [30]. In E16K/E61K Fld tight non-crystallographic restraints between the four different protein chains of the asymmetric unit were applied during refinement, which were gradually loosened in the final rounds. Stereochemistry of the models was checked using PROCHECK [31]. Atomic coordinates are deposited at the PDB: 3esz for K2A/K3A Fld, 3esy for E16K/E61K Fld and 3esx for E16K/E61K/D126K/D150K Fld.

Electrostatic potential surface and dipole moment calculations.

In silico Fld mutant models, based on the *Anabaena* WT Fld structure (PDB 1flv), were generated using the mutation tool implemented in SPDB-Viewer 3.7 [32]. Energy minimization was done using the AMBER suite of molecular dynamics simulations and the amber force field [13, 33]. The partial charge on each FMN atom was taken from [34]. The H++ server was used to protonate hydrolysable residues [35]. R.m.s.d. values for all atoms of modelled molecules with regard to WT were under 0.2 Å [13]. Molecular surfaces with electrostatic potential were calculated with PyMol [28]. The dipole moment (μ) for WT and mutated Flds was calculated by using the equation $\mu = \sum q_i r_i$; q_i being the partial charge and r_i the coordinates of each protein atom. The centre of mass of each protein was used as the reference position for calculation of μ [13].

RESULTS

Expression, purification and spectral properties of the Fld mutants.

Absorbance spectra of the Fld mutants were similar to those of WT Fld (Table SP2), indicating that they fold and bind FMN without major structural perturbations.

The flavin extinction coefficients only slightly differed from that of the WT Fld, and changes were measurable only for the D144A Fld.

Midpoint reduction potentials

Flds containing individual charge reversal replacements at positions 12, 16, 20, 67 or 126, as well as the E16K/D126K and E16K/E20K/D126K multiple mutants, only produced minor effects on $E_{ox/sq}$ and $E_{sq/hq}$ (Table 1, Figure 1). However, E61K, E16K/E61K and E16K/E61K/D126K/D150K displaced $E_{ox/sq}$ to considerably more negative values, whereas $E_{sq/hq}$ was less negative (Figure 1). Such displacements explained the decrease in the amount of the maximal semiquinone stabilised by these mutants (Table SP2). Replacement of D144 with Ala produced a Fld with a $E_{sq/hq}$ considerably less negative than WT Fld. Again, this correlated with a considerably decrease in the maximal amount of semiquinone stabilised. Finally, simultaneous replacement of the N-terminal lysines with either Ala or Glu moderately influenced less negative $E_{ox/sq}$ values, but had not effect on $E_{sq/hq}$.

Interaction of Fld_{ox} variants with FNR_{ox}

The spectral changes elicited upon titration of FNR_{ox} with the Fld_{ox} mutants were in general similar to those reported for the interaction of WT proteins. However, titrations with T12K and D144A showed displacements of the flavin Band-II (Figure 2A, Table 2), suggesting slight different environments for the FAD-FMN interaction [14]. No difference spectra were observed when titrating FNR with E16K/E20K/D126K or E16K/E61K/D126K/D150K Flds. Thus, combination of these mutations prevented the FNR-Fld interaction through their flavins. The E67A, D126K, K2A/K3A and K2E/K3E Flds interaction parameters with FNR were similar to those reported for WT Fld (Figure 2B, Table 2). E20K, E61K and E16K/D126K mutations induced a slight weakening of the FNR_{ox} : Fld_{ox} interaction. 14- to 18-fold weaker

complexes were observed with E16K and E16K/E61K Flds and, up to 23- and 36-fold weaker ones with T12K and D144A, respectively (Table 2). In general, extinction coefficient changes ($\Delta\epsilon$) were within a factor of 2 of the WT Fld complex (Table 2). However, $\Delta\epsilon$ slightly increased beyond that factor for the titration with D144A, while a decrease was observed for the double E16K/E61K and E16K/D126K mutants. These later observations suggest slight different relative interactions between the flavin centres with regard to those found in the WT complex.

Steady-state kinetic parameters for WT FNR when using the Fld mutants as electron carriers.

The FNR cytochrome *c* reductase activity [25] was assayed using the different Flds to investigate whether the introduced mutations modulate the Fld ability to interact and to exchange electrons with FNR and Cytc (Table 2). E16K/E20K/D126K and E16K/E61K/D126K/D150K Flds presented low efficiency exchanging electrons between FNR and Cytc as consequence of very high K_m^{Fld} values. However, the use of D144A and E67A Flds slightly improved the FNR k_{cat} (Table 2), suggesting that these mutants have improved either their abilities as FNR electron acceptors and/or as Cytc electron donors. In general, the mutations produced larger K_m^{Fld} values, with the only exception of D126K Fld (Table 2). FNR K_m^{Fld} increased by a factor of 3-fold when using T12K, E67A, D144A and E16K/E61K Flds or 5-fold with E20K, E61K and E16K/D126K Flds. Combination of both effects produced significant differences in the FNR catalytic efficiency (k_{cat}/K_m) (Table 2), but the single D126K mutant was the only that led to an increased efficiency apparently due to the formation of stronger interactions. In conclusion, the use of E20K, E61K, E16K/D126K, E16K/E20K/D126K and especially E16K/E20K/D126K or E16K/E61K/D126K/D150K Flds considerably

hindered the efficiency of the ET process from FNR to Cytc, most likely due to weaker productive interactions between these Fld variants and FNR.

Pre-steady-state kinetic analysis of the ET from Fld_{hq} mutants to $Cytc_{ox}$.

To elucidate if changes observed in FNR catalytic efficiency could be due to a less efficient interaction and ET between Fld and Cytc, ET from the Fld_{hq} mutants to $Cytc_{ox}$ was analysed by stopped-flow. Similar two-exponential kinetics to those for the $Cytc_{ox}$ reduction by WT Fld were observed for the Fld mutants [18]. Processes with E16K, E67A, D126K, D144A, K2A/K3A and K2E/K3E Fld_{hq} s presented k_{ap} values within a factor of two of WT Fld_{hq} (Table 3), indicating that these residues do not play a major role in the optimal Cytc-Fld interaction. However, E16K/E61K, E16K/D126K, E16K/E20K/D126K and, especially T12K and E16K/E61K/D126K/D150K Fld_{hq} s transferred electrons to $Cytc_{ox}$ with slower rates (Table 3).

Pre-steady-state kinetic analysis of the ET processes between FNR and Fld mutants.

When following the time course of the physiological ET reaction, from Fld_{hq} to WT FNR_{ox} , processes with T12K, E67A, D126K and K2E/K3E Flds showed WT behaviour (Table 3 and Figures 3A and 3B). Kinetic traces for these reactions fit a two step process: formation of the semiquinones of both proteins, followed by further reduction of FNR_{sq} to the fully reduced state by a second Fld_{hq} molecule [14]. The reaction between the WT proteins takes place mainly within the instrumental dead time (~ 2 ms) and therefore, k_{ap2} cannot be separated from k_{ap1} [25]. However, the process was reported considerably slower for some mutants, allowing the determination of the two rate constants separately [14, 20, 25]. Processes with the remaining mutants were slower and different behaviours could be observed. The E16K and, particularly, the K2A/K3A Flds despite showing slower k_{ap1} and k_{ap2} parameters were still able to reduce FNR (Table 3, Figures 3A and 3B). Combined charge reversal mutations around the

FMN hindered ET from Fld_{hq} to FNR_{ox} , the effect being particularly patent in E16K/E61K/D126K/D150K Fld. The process was also hindered with D144A. The amplitudes of the kinetic traces were in general similar for the different Fld variants. The only exception was the reduction of FNR_{ox} by D144A Fld_{hq} that took place in considerably lower extent (Figure 3A).

The reverse reaction, WT FNR_{hq} with WT Fld_{ox} , has been shown as a relatively slow two-step process due to initial production of Fld_{sq} and FNR_{sq} , followed by the reduction of a second Fld_{ox} molecule by the FNR_{sq} produced in the first step [14, 20, 25]. The kinetic traces for the reaction of all Fld_{ox} mutants also fit a biphasic process (Figure 3C and 3D). In general, k_{ap1} values were within a factor of 2 of that with WT Fld_{ox} . However, E67A, E16K/E61K and, especially, T12K appear more efficient accepting electrons from FNR, while a hindering effect was observed for D144A, E16K/E126K and E16K/E61K/D126K/D150K (Table 3). k_{ap2} values were especially slower for E16K, D144A and the mutants containing simultaneous replacements of negatively charged residues. The amplitudes of the traces were in general similar or within a factor of 1.5 larger than those observed for the reaction with WT Fld_{ox} .

Pre-steady-state kinetic analysis of the reduction of Fld variants by PSI.

Reduction of Fld_{ox} to the semiquinone state by PSI_{rd} using laser-flash absorption spectroscopy has demonstrated to be a useful model to analyse the interaction forces and ET parameters involved in the physiological reaction [5, 13, 14, 20]. In addition, and although the $\text{Fld}_{\text{sq}}/\text{Fld}_{\text{hq}}$ couple is with no doubt involved in shuttling electrons between PSI and FNR, a physiological role for the $\text{Fld}_{\text{ox}}/\text{Fld}_{\text{sq}}$ couple can not be precluded [5, 7]. All Fld mutants showed monoexponential kinetic traces when reduced by PSI_{rd} , as reported for WT Fld [3]. The k_{obs} for the reduction of WT, T12K, E67A, E16K/E61K/D126K/D150K and K2A/K3A Fld_{ox} depended non-linearly on the Fld

concentration, showing a saturation profile (Figures 4A and 4B). This suggests that a transient bimolecular $\text{PSI}_{\text{rd}}:\text{Fld}_{\text{ox}}$ complex is formed prior to ET [4, 36], although different explanations for this type of saturation profiles have also been given [37]. From the non-linear dependence of k_{obs} vs Fld concentration, minimal values for both the K_d and the ET first-order rate constant (k_{et}) can be inferred (Figures 4A and 4B, Table 4). Replacement of T12 with Lys only slightly increased the affinity of Fld_{ox} by PSI_{rd} , but hindered its ability to accept electrons from PSI_{rd} . On the contrary, the simultaneous introduction of two Ala at K2 and K3 produced a 3-fold decrease of the complex affinity, but enhanced the ET rate. Noticeably, simultaneous replacement with Lys of positions 16, 61, 126 and 150 produced a Fld that accepts the electron twice faster (Figure 4B, Table 4). The remaining mutants showed a linear dependence of k_{obs} on Fld concentration (Figures 4A and 4B). This indicates that PSI_{rd} and these Fld_{ox} mutants reacted, under the assayed conditions, through a collisional type mechanism without detectable transient complex formation. Second order bimolecular rate constants (k_2) for Fld reduction can be estimated from the linear plots (Table 4). Although the observed linear dependences indicated that the equilibrium constant for complex formation was decreased, the k_{obs} values obtained at high Fld concentration were similar or even considerably higher (see the E16K/D126K, D144A and, particularly, E16K/E61K in Figures 4A and 4B and Table 4) than those exhibited by WT Fld. In contrast, E16K/E20K/D126K Fld was unable to accept one electron from PSI (Figure 4B, Table 4).

The k_{obs} profiles determined at varying MgCl_2 concentrations presented in general a biphasic dependence (Figures 4C and 4D), as reported for the WT protein [3, 14]. This bell-shaped salt dependence is explained as the initially formed electrostatic interaction being not the optimal for ET, requiring thus a rearrangement that could be

prevented by the strong electrostatic forces acting at low ionic strength [3]. The E16K/E61K and E16K/E61K/D126K/D150K profiles indicate a shift of the maximum k_{obs} to a lower MgCl₂ concentration. Therefore, for these particular variants the most efficient orientation for ET is obtained at lower ionic strengths, at which higher efficiencies than for the WT are observed. Moreover, despite E16K/E20K/D126K Fld kept its low efficiency through the whole salt concentration range, it also showed a maximum at lower ionic strength than WT (Figure 4D). On the contrary, k_{obs} for T12K Fld was considerably enhanced with increasing MgCl₂ concentrations, reaching similar values to WT Fld at the highest concentrations studied and showing a displacement of k_{obs} maximum to higher ionic strengths (Figure 4C). These data suggest that T12K favours a strong non-productive interaction at low ionic strength, but it does not prevent Fld from accepting electrons from PSI when the strong electrostatic interaction is abolished.

Structures of the K2A/K3A, E16K/E61K and E16K/E61K/D126K/D150K Flds

The E16K/E61K Fld crystal structure had four Fld monomers in the asymmetric unit (Table SP1), which were overall similar among them (r.m.s.d. 0.40 Å for C α) and with WT Fld (0.46, 0.44, 0.44 and 0.51 Å for A, B, C, and D monomers, respectively). Monomer A showed a *cis*-isomer of the N58-I59 peptide bond (Figure SP2A), apparently due to the insertion of Tyr49, from a symmetry related monomer, between I59 and the isoalloxazine (Figure SP2A). The conformation of the *cis*-bond was stabilised by a H-bond between the NH of residue 60 and a water molecule that bridges with the N5 of the isoalloxazine through a second H-bond. The crystal packing does not affect the conformation of this loop in B, C and D, which retain the *trans* isomer as in WT Fld. Nevertheless, the distance between the isoalloxazine N5 and the NH of I59 slightly differs among B, C and D monomers (between 3.30 and 3.68 Å).

E16K/E61K/D126K/D150K Fld presented two monomers in the asymmetric unit (Table SP1). None of the four replacements provoked a significant change in the $\text{C}\alpha$ backbone configuration (r.m.s.d. with regard to WT Fld 0.45 and 0.66 Å for A and B monomers, respectively), despite the orientation of the introduced Lys chains was different from those of the replaced residues. These changes in orientation are often observed in residues facing the solvent. The conformation of the 50's loop was conserved in the mutant, being the H-bond between the N5 atom of the isoalloxazine ring of FMN and the N atom of I59 0.16 Å shorter than in WT Fld (Figure SP2B).

The K2A/K3A Fld structure contained two Fld monomers in the asymmetric unit (Table SP1). Both subunits presented a similar conformation between them (r.m.s.d. 0.39 Å) and with WT Fld (0.49 and 0.42 Å for A and B, respectively) (Figure 5A). Monomer A presented a *cis* disposition for the N58-I59 peptide bond that was not stabilised by any interaction between atoms of the 50's loop and the N5 of the FMN isoalloxazine ring. In monomer B, the conformation of the 50's loop remained essentially as in WT Fld. The H-bond between the isoalloxazine N5 and HN of I59 (3.34 Å) is shorter than in WT (3.71 Å). An additional consequence of the different configuration of 59-60 loop between monomers is that the NH of residue 60 in B is closer to the O4 atom of the isoalloxazine (2.74 Å, similar to that of WT Fld of 2.79 Å) than in A (3.04 Å).

DISCUSSION

Fld must interact with PSI and FNR in such a way that its FMN cofactor faces towards the F_B [4S-4Fe] of PsaC in PSI or the FAD in FNR. The role of the Fld charge distribution in the optimal orientation of the protein, particularly of its FMN group, has been analysed.

Effects of mutations on the Fld midpoint potentials.

$E_{ox/sq}$ was only considerably altered for E61K, E16K/E61K and E16K/E61K/D126K/D150K Flds (Table 1). This confirms replacement of E61 as the major determinant for the observed changes. Transition from the oxidised to the semiquinone in some Flds is accompanied by a backbone peptide rearrangement that provides a versatile device for $E_{ox/sq}$ manipulation [15, 38]. In *Anabaena* Fld this corresponds to the 58-59 peptide bond. In the oxidised state the amide of I59 establishes a weak H-bond with the N5 of the flavin ring, “O-down” conformation. This bond is proposed to flip to an “O-up” conformation upon reduction to the semiquinone, involving the breaking of the above mentioned H-bond in favour of the formation of a stronger one between the carbonyl of N58 and N5H of FMN [13, 38]. The more negative $E_{ox/sq}$ in E61K, E16K/E61K and E16K/E61K/D126K/D150K Flds are consistent with a less favourable thermodynamic conversion to the semiquinone (Table 1). The shorter N5-HN59 H-bond observed in these $Fld_{ox/sq}$ (Figure SP2), suggests an increase in the conformational energy of the N58-I59 bond that favours the “O-down” conformation. Therefore, E61 appears among the chains whose nature influences the “O-down to O-up” conformational change on one electron reduction of Fld_{ox} , making reduction more or less difficult and shifting $E_{ox/sq}$ to more or less negative values [13, 15, 19, 39, 40]. Surprisingly, the K2A/K3A and K2E/K3E Flds had slightly less negative $E_{ox/sq}$ values, despite their mutations being more than 30 Å away from FMN (Figure 5B). However, they considerably decrease the magnitude of the Fld dipole moment changing also its direction (Figure 6, Table SP3). The structure of K2A/K3A Fld also shows a possible relative orientation between the flavin and the 58-59 backbone that does not stabilise the H-bond with the N5 of FMN (Figure 5A, monomer A), thus favouring the reduction. Therefore, the structural flexibility in the 58-59 bond

and the modulation of the distance between it and the N5 of the flavin support a function of this loop in the regulation of the $E_{ox/sq}$ in *Anabaena* Fld.

$E_{sq/hq}$ was in general not influenced by the introduced mutations (Table 1). However, in D144A, E61K, E16K/E61K and E16K/E61K/D126K/D150K $E_{sq/hq}$ shifted considerably. Since the FMN_{hq} in Fld is normally not protonated at N1, repulsive forces are generated in the negatively charged protein environment and electrostatic interactions are a determinant factor for the low $E_{sq/hq}$ [15, 41]. The influence of charged residues depends on the distance and on the relative location to the isoalloxazine [15, 19]. The decrease of the negative electrostatic potential around the flavin ring introduced by replacement of E61 (7 Å away from the ring) appears as the main cause of the displacement of $E_{sq/hq}$ to less negative values in E61K, E16K/E61K and E16K/E61K/D126K/D150K Flds (Figure 5B). Replacement of D144 with Ala also had a remarkable effect on $E_{sq/hq}$. D144 contributes, together with D90, E145 and D146, to a negatively charged patch situated less than 6 Å from the isoalloxazine N1 (Figure SP3). D144 is not solvent accessible or in direct contact with the flavin, but the electrostatic repulsion of its side chain appears to force those of D90 and D146 towards the isoalloxazine. Replacement of D144 with Ala must allow a retraction of D90 and D146 towards the position of D144 in WT Fld (Figure SP3). This will allow a better neutralisation of the hydroquinone negative charge and therefore, a less negative $E_{sq/hq}$ [15]. Displacement of D90 and D146 chains might also increase the FMN solvent accessibility, a factor that contributes also to $E_{sq/hq}$ by making it less negative [15, 42].

Effects of mutations on the Fld interaction and ET with FNR

The single mutations introduced at T12, E16, E67, D126 and D144, despite the negative influence on the interaction produced in some cases (T12K, E16K, D144A) (Table 2), generally allowed the exchange of electrons between Fld and FNR or Cyt_c

(Tables 2 and 3). k_{cat} and k_{ap} values for these ET processes were in many cases modulated, either positively or negatively. Since these mutations did not produce major changes in the thermodynamics (Table 1), the kinetic effects must be due to the difference in the strength of the interaction, caused by small changes in their electrostatic surface potentials and in the orientation and magnitude of their molecular dipole moments (Figure SP4, Table SP3). Therefore, these positions appear far from being critical by their own for the interaction and ET between Fld and FNR. The only exception is D144A Fld. This mutation prevents the physiological ET from Fld_{hq} to FNR (Table 3, Figure 3). The explanation must be found in its $E_{\text{sq/hq}}$ that makes the ET from Fld_{hq} to FNR much less favourable from the thermodynamic point of view.

Among the mutants produced by simultaneous replacements at E16, E61, D126 or D150, only E16K/E61K and E16K/D126K produced complexes with FNR. The strength of these interactions was similar to that of the single E16K variant, but $\Delta\epsilon$ suggests considerably smaller degrees of interaction between the flavins (Figure 2, Table 2). These Fls appear still able to accept electrons from FNR (Table 3, Figure 3), but the decrease in the strength of the interaction with FNR and in the ET efficiency with Cyt c makes them poor electron carriers (Tables 2 and 3). Additionally, all these mutants, but particularly E16K/E61K/D126/D150K, have lost the ability to efficiently reduce FNR (Table 3). More positive $E_{\text{sq/hq}}$ values might somehow contribute to the behaviour of E16K/E61K and E16K/E61K/D126/D150K Fls, but not to the other two mutants. Important changes in their electrostatic potential surfaces are observed, which influence changes in the orientation and magnitude of their molecular dipole moments (Table SP3, Figures 5B and 6). Thus, while in WT Fld and the single mutants the negative end of the dipole moment points towards the flavin ring, the negative end of E16K/E61K/D126/D150K is not anymore oriented towards it (Figure 6A). In fact, if

docking between this mutant and FNR would still have to occur through the alignment of their respective dipole moments, this mutant would never face the FAD cofactor of FNR through its FMN surface (Figures 6B and 6C). This is consistent with the lack of interaction between FMN and FAD observed when titrating FNR with this mutant. Surprisingly, as above mentioned, these Flds were still able to accept electrons from FNR. Despite that the thermodynamic parameters favour the process, the observed reaction might only correlate with a collisional-type reaction. This agrees with the proposal of alternative productive binding modes between FNR and Fld [19, 21].

K2A/K3A and K2E/K3E Flds have an almost WT behaviour, the only difference being the slightly reduced k_{ap} when accepting electrons from FNR (Table 3). Minor effects should be expected from the reaction thermodynamic driving force (Table 1). The explanation should be again found in the decrease of the Fld dipole moment magnitude and the change in its direction towards the FMN phosphate group (Figure 6).

Effects of mutations on the ET from PSI to Fld.

For many of the mutants ET from PSI_{rd} to Fld_{ox} takes place through a collisional-type mechanism (Table 4, Figure 4). These data indicate that E16, D126 and D144 play some role in the formation of ET complexes with PSI. Noticeably, the k_{obs} values for E16K/E61K are higher than those obtained for WT (Figure 4). This was already described when producing single mutants at E61 [20]. It indicates that E61 contributes to the orientation of Fld on the PSI docking site, producing a WT complex that is not the optimal for ET. For the rest of the mutations k_{obs} at a given concentration is lower than for WT Fld. Since the introduced mutations are not in the direct coordination of the isoalloxazine this can hardly be the consequence of a different structural FMN environment affecting the ET mechanism, but rather due to an

orientation between the protein dipoles not optimal for ET or, to the change in the protein electrostatic potential (Figures 5B and 6).

T12K, E67A, E16K/E61K/D126K/D150K and K2A/K3A Flds accept electrons from PSI following transient complex formation [3, 14]. The $\text{PSI}_{\text{rd}}:\text{T12K Fld}_{\text{ox}}$ complex, despite being stronger than that for WT Fld, is not optimal for ET. Introduction of a Lys at position 12 is not expected to influence the orientation of the molecular dipole moment, but will induce changes in the electrostatic potential favouring a complex less efficient for ET (Figure SP4). Similar results were reported when replacing T12 with Val, suggesting this Thr as a key residue in this process [20]. Binding ability of E16K/E61K/D126K/D150K Fld to PSI is not sensibly affected, but k_{et} is considerably enhanced. The more negative $E_{\text{ox/sq}}$ of E16K/E61K/D126K/D150K Fld (-41 mV) might influence its kinetic behaviour by decreasing the driving force of its reduction. The change in the orientation of the molecular dipole moment (Figure 6) is expected to have also a negative effect. Complex formation with PSI is slightly impaired in K2A/K3A Fld mutant, but the k_{et} for its reduction is again enhanced (Table 4). This region of Fld is not expected to be involved in the interaction with PSI and the differences can not be due to changes in the isoalloxazine environment. However, removal of these two Lys considerably reduced the magnitude of the Fld dipole moment and changes its orientation (Figure 6, Table SP3). Therefore, the increased efficiency of E16K/E61K/D126K/D150K and K2A/K3A Flds in accepting electrons from PSI has to be related to different orientations of these Flds at the donor site of PSI. The exact localisation of the protein acceptor on the PSI is still far to be determined. Moreover, the orientation of the protein carrier on the PSI docking site might be different in plants and cyanobacteria. Additionally, PSI in cyanobacteria has also different arrangements

when grown under iron deficient conditions [43]. Therefore, *in vivo* a variability of these interactions will be also occurring.

Electrostatic non-specific interactions as major determinants of the efficient interaction between Fld and its counterparts.

The Fld interaction with FNR is confirmed to be less specific than that of Fd, and apparently more than one orientation in the encounter complex can be efficient. Additionally, some of the specific introduced mutations in Fld favour single orientations which improve association and ET with a particular partner. This suggests that the flavin atoms might be those mainly involved in the interaction, as suggested by docking analysis [21], and probably the only ones directly responsible for ET. Subtle changes at the isoalloxazine environment influence the Fld binding abilities and modulate the ET processes by producing different orientations and distances between the redox centres. This confirms that Fld interacts with different structural partners through non-specific interactions. This promiscuity, in turn decreases the potential efficiency in ET that could be achieved if unique favourable orientations were produced with a reduced number of partners [19]. Heterogeneity of ET kinetics is an intrinsic property of Fld reduction, and can be most probably ascribed to different conformations of the PSI:Fld and FNR:Fld complexes [5, 21]. Therefore ET reactions involving Fld might not have as much specific interaction requirements as other reactions involving protein-protein interactions and, the bound state could be formed by dynamic ensembles instead of single conformations as has already been observed in other ET systems [44, 45]. During Fld-dependent photosynthetic ET, the Fld molecule must pivot between its docking site on PSI to that on FNR. Formation of transient complexes is useful during this process, though not critical, for promoting efficient reduction of Fld and FNR and for avoiding reduction of oxygen [5, 19]. The electrostatic alignment appears as one of

the major determinants of the orientation of Fld on the partner surfaces. Fld-domains and FNR-domains in dual-flavin reductases appear to have eliminated the pressure to maintain strong contacts and the dipole moment alignment between the domains [46-48]. However, the negatively charge residues analysed in this work are also conserved in their Fld-domains (Figure SP1C). Part of the role of these residues might have been conserved upon evolution to orientate the Fld-domain when pivoting between the FNR-domain and their electron acceptors [47]. Finally, the fact that the same replacements on the Fld surface did not similarly hinder or enhance processes with PSI and FNR also suggests a different interaction mode with both partners. Such modes can differ in the Fld surfaces in contact with both protein partners. These assumptions are also justified by considering the large number of negative charges borne by Fld, which should make its electrostatic steering on the positively charged FNR and, particularly, on the large PSI docking site, relatively insensitive to small changes in the Fld charge.

Acknowledgments

This work has been supported by Spanish Ministry of Education and Science (BIO2007-65890-C02-01 to M.M.) and DGA (Grant PM062/2007 to M.M.). We thank to Dr. JM Mancheño for his helpful assistance during X-ray data collection at the BM16 beamline of the ESRF.

Abbreviations: ET, electron transfer; Fd, Ferredoxin; Fld, Fld_{ox}, Fld_{sq}, Fld_{hq}, Flavodoxin and in its oxidised, semiquinone and hydroquinone states, respectively; FNR, FNR_{ox}, FNR_{sq}, FNR_{hq}, Ferredoxin-NADP⁺ reductase and in its oxidised, semiquinone and hydroquinone states, respectively; ApoFld, apoflavodoxin; K_d , dissociation constant; k_{ap} , apparent rate constant; k_{et} , first-order electron transfer rate constant; k_{obs} , pseudo first-order observed rate constant; k_2 , second order rate constant; PSI, PSI_{ox}, PSI_{rd}, Photosystem I and in its oxidised and reduced states, respectively; WT, wild-type; Cyt_c,

Cyt_{c_{ox}}, Cyt_{c_{rd}}, horse heart cytochrome *c* and in its oxidised and reduced states, respectively.

REFERENCES

- [1] M. Medina and C. Gómez-Moreno, Photosynth Res 79 (2004) 113-131.
- [2] G.M. Ullmann, M. Hauswald, A. Jensen and E.W. Knapp, Proteins 38 (2000) 301-309.
- [3] M. Medina, M. Hervás, J.A. Navarro, M.A. De la Rosa, C. Gómez-Moreno and G. Tollin, FEBS Lett 313 (1992) 239-242.
- [4] J.A. Navarro, M. Hervás, C.G. Genzor, G. Cheddar, M.F. Fillat, M.A. de la Rosa, C. Gómez-Moreno, H. Cheng, B. Xia, Y.K. Chae and et al., Arch Biochem Biophys 321 (1995) 229-238.
- [5] P. Sétif, Biochim Biophys Acta 1507 (2001) 161-179.
- [6] P. Jordan, P. Fromme, H.T. Witt, O. Klukas, W. Saenger and N. Krauss, Nature 411 (2001) 909-917.
- [7] P. Sétif. in (Golbeck, J.H., ed.) Photosystem I. The light-driven platocyanin:ferredoxin oxidoreductase, Springer, Dordrecht, The Netherlands 2006, pp. 439-454.
- [8] N. Fischer, M. Hippler, P. Sétif, J.P. Jacquot and J.D. Rochaix, Embo J 17 (1998) 849-858.
- [9] J. Hanley, P. Sétif, H. Bottin and B. Lagoutte, Biochemistry 35 (1996) 8563-8571.
- [10] V.P. Chitnis, Y.S. Jungs, L. Albee, J.H. Golbeck and P.R. Chitnis, J Biol Chem 271 (1996) 11772-11780.
- [11] P. Barth, I. Guillouard, P. Sétif and B. Lagoutte, J Biol Chem 275 (2000) 7030-7036.
- [12] N. Krauss, W. Hinrichs, I. Witt, P. Fromme, W. Pritzkow, Z. Dauter, C. Betzel, K.S. Wilson, H.T. Witt and W. Saenger, Nature (1993) 326-331.
- [13] S. Frago, G. Goñi, B. Herguedas, J.R. Peregrina, A. Serrano, I. Pérez-Dorado, R. Molina, C. Gómez-Moreno, J.A. Hermoso, M. Martínez-Júlvez, S.G. Mayhew and M. Medina, Arch Biochem Biophys 467 (2007) 206-217.
- [14] J.L. Casaus, J.A. Navarro, M. Hervás, A. Lostao, M.A. De la Rosa, C. Gómez-Moreno, J. Sancho and M. Medina, J Biol Chem 277 (2002) 22338-22344.

- [15] I. Nogués, L.A. Campos, J. Sancho, C. Gómez-Moreno, S.G. Mayhew and M. Medina, *Biochemistry* 43 (2004) 15111-15121.
- [16] J.K. Hurley, R. Morales, M. Martínez-Júlvez, T.B. Brodie, M. Medina, C. Gómez-Moreno and G. Tollin, *Biochim Biophys Acta* 1554 (2002) 5-21.
- [17] R. Morales, M.H. Charon, G. Kachalova, L. Serre, M. Medina, C. Gómez-Moreno and M. Frey, *EMBO Rep* 1 (2000) 271-276.
- [18] I. Nogués, M. Martínez-Júlvez, J.A. Navarro, M. Hervás, L. Armenteros, M.A. de la Rosa, T.B. Brodie, J.K. Hurley, G. Tollin, C. Gómez-Moreno and M. Medina, *Biochemistry* 42 (2003) 2036-2045.
- [19] G. Goñi, A. Serrano, S. Frago, M. Hervás, J.R. Peregrina, M.A. De la Rosa, C. Gómez-Moreno, J.A. Navarro and M. Medina, *Biochemistry* 47 (2008) 1207-1217.
- [20] I. Nogués, M. Hervás, J.R. Peregrina, J.A. Navarro, M.A. de la Rosa, C. Gómez-Moreno and M. Medina, *Biochemistry* 44 (2005) 97-104.
- [21] M. Medina, R. Abagyan, C. Gomez-Moreno and J. Fernandez-Recio, *Proteins* 72 (2008) 848-862.
- [22] M. Hervás, J.M. Ortega, J.A. Navarro, M.A. De la Rosa and H. Bottin, *Biochim Biophys Acta* 1184 (1994) 235-241.
- [23] D.I. Arnon, *Plant Physiol* 24 (1949) 1-15.
- [24] S.G. Mayhew and V. Massey, *J Biol Chem* 244 (1969) 794-802.
- [25] M. Medina, M. Martínez-Júlvez, J.K. Hurley, G. Tollin and C. Gómez-Moreno, *Biochemistry* 37 (1998) 2715-2728.
- [26] Z. Otwinowski and W. Minor, *Methods in Enzymology* 276 (1997) 307-326.
- [27] A. Vagin and A. Teplyakov, *J. Appl. Cryst.* 30 (1997) 1022-1025.
- [28] A.T. Brunger, P.D. Adams, G.M. Clore, W.L. DeLano, P. Gros, R.W. Gross-Kunstleve, J.S. Jiang, J. Kuszewski, M. Nilges, N.S. Pannu, R.J. Read, L.M. Rice, T. Simonson and G.L. Warren, *Acta Crystallogr D Biol Crystallogr* 54 (1998) 905-921.
- [29] G.N. Murshudov, A.A. Vagin and E.J. Dodson, *Acta Crystallogr D Biol Crystallogr* 53 (1997) 240-255.
- [30] T.A. Jones, J.Y. Zou, S.W. Cowan and M. Kjeldgaard, *Acta Crystallogr A* 47 (Pt 2) (1991) 110-119.
- [31] R.A. Laskowski, M.W. MacArthur, D.S. Moss and J.M. Thornton, *J. Appl. Cryst.* 26 (1993) 283-291.

- [32] N. Guex and M.C. Peitsch, *Electrophoresis* 18 (1997) 2714-2723.
- [33] D.A. Case, T.E. Cheatham, T. Darden, H. Gohlke, R. Luo, K.M. Merz, A. Onufriev, C. Simmerling, B. Wang and R.J. Woods, *J Comput Chem* 26 (2005) 1668-1688.
- [34] C. Schneider and J. Suhnel, *Biopolymers* 50 (1999) 287-302.
- [35] J. Myers, G. Grothaus, S. Narayanan and A. Onufriev, *Proteins* 63 (2006) 928-938.
- [36] U. Muhlenhoff and P. Sétif, *Biochemistry* 35 (1996) 1367-1374.
- [37] D.M. Tiede, A.C. Vashishta and M.R. Gunner, *Biochemistry* 32 (1993) 4515-4531.
- [38] M. Kasim and R.P. Swenson, *Biochemistry* 40 (2001) 13548-13555.
- [39] M.L. Ludwig, K.A. Patridge, A.L. Metzger, M.M. Dixon, M. Eren, Y. Feng and R.P. Swenson, *Biochemistry* 36 (1997) 1259-1280.
- [40] W. Watt, A. Tulinsky, R.P. Swenson and K.D. Watenpaugh, *J Mol Biol* 218 (1991) 195-208.
- [41] Z. Zhou and R.P. Swenson, *Biochemistry* 35 (1996) 15980-15988.
- [42] R.P. Swenson and G.D. Krey, *Biochemistry* 33 (1994) 8505-8514.
- [43] J. Nield, E.P. Morris, T.S. Bibby and J. Barber, *Biochemistry* 42 (2003) 3180-3188.
- [44] J.A. Worrall, W. Reinle, R. Bernhardt and M. Ubbink, *Biochemistry* 42 (2003) 7068-7076.
- [45] P.B. Crowley and M.A. Carrondo, *Proteins* 55 (2004) 603-612.
- [46] M. Wang, D.L. Roberts, R. Paschke, T.M. Shea, B.S. Masters and J.J. Kim, *Proc Natl Acad Sci U S A* 94 (1997) 8411-8416.
- [47] K.R. Wolthers, X. Lou, H.S. Toogood, D. Leys and N.S. Scrutton, *Biochemistry* 46 (2007) 11833-11844.
- [48] E.D. Garcin, C.M. Bruns, S.J. Lloyd, D.J. Hosfield, M. Tiso, R. Gachhui, D.J. Stuehr, J.A. Tainer and E.D. Getzoff, *J Biol Chem* 279 (2004) 37918-37927.
- [49] S.G. Mayhew, *Methods Mol Biol* 131 (1999) 49-59.

Table 1: Midpoint reduction potentials for the different *Anabaena* Fld forms.

Data obtained in 50 mM Tris/HCl at pH 8.0 and 25 °C.

Fld form	$E_{\text{ox/sq}}$ (mV)	$E_{\text{sq/hq}}$ (mV)	$\Delta E_{\text{ox/sq}} - \Delta E_{\text{ox/sq}}^{\text{WT}}$ (mV)	$\Delta E_{\text{sq/hq}} - \Delta E_{\text{sq/hq}}^{\text{WT}}$ (mV)
WT ^a	-256	-445	-	-
T12K ^b	-252	-438	4	7
E16K ^b	-254	-440	2	5
E20K ^a	-265	-430	-9	15
E61K	-298	-399	-42	46
E67A	-258	-457	-2	-12
D126K	-254	-451	2	-6
D144A	-248	-375	8	70
E16K/E61K	-301	-390	-45	55
E16K/D126K	-253	-440	3	5
E16K/E20K/D126K	-255	-438	1	7
E16K/E61K/D126K/D150K	-297	-391	-41	54
K2A/K3A	-238	-445	18	0
K2E/K3E	-232	-444	24	1
FMN free ^c	-365	-117	-109	328

^a Data were according to those previously published [15]. Reproducible WT data have been again obtained in the present work as control.

^b Data from [13].

^c Calculated as described [15, 49] (pH 8.0 and 25°C).

Table 2: Steady-state parameters for the *Anabaena* PCC 7119 Fld-FNR interaction. Dissociation constants, extinction coefficient changes at band-I, position of flavin bands in the difference spectra and free energy for complex formation of WT FNR_{ox} with WT and mutated Fld_{ox} forms and kinetic parameters for the FNR NADPH-dependent cytochrome *c* reductase activity using the different Fld variants.

Fld form	K_d (μM)	$\Delta\epsilon_{\text{band-I}}$ ($\text{M}^{-1}\text{cm}^{-1}$)	Band-II (nm)	Band-I (nm)	ΔG° (kcal mol $^{-1}$)	$k_{\text{cat}}^{\text{Fld}}$ (s^{-1})	K_m^{Fld} (μM)	$k_{\text{cat}}/K_m^{\text{Fld}}$ ($\mu\text{M}^{-1}\text{s}^{-1}$)
WT ^a	2.6	1.5	394	465	-7.5	23.3	33.0	0.70
T12K	60	1.5	386	463	-5.8	24.9	78.6	0.32
T12V ^b	2.2	1.4	394	465	-7.8	11.0	11.1	1.00
E16K	37	1.2	394	464	-6.0	18.6	33.7	0.55
E20K ^b	14.5	2.4	394	465	-6.6	25.0	172	0.14
E61K ^b	11	2.9	394	465	-6.8	31.3	166	0.19
E67A	3.0	1.9	390	462	-7.5	65.5	97.9	0.67
D126K	4.2	2.1	390	464	-7.3	23.5	12.2	1.93
D144A	94	3.6	382	465	-5.5	58.2	90.1	0.65
E16K/E61K	46	0.4	398	460	-5.9	39.3	91.4	0.43
E16K/D126K	19	0.6	398	463	-6.4	24.8	171	0.14
E16K/E20K/D126K	c	c	c	c		d	d	d
E16K/E61K/D126K/D150K	c	c	c	c		e	>400 ^e	e
K2A/K3A	5.3	2.0	392	465	-7.2	28.5	49.2	0.58
K2E/K3E	4.3	1.8	392	465	-7.2	22.4	32.0	0.70

^a Data were according to those previously published [25].

^b Data from [20].

^c Difference spectra were not observed.

^d The dependence of the kinetic on [Fld] was linear with a $k = 5.0 \times 10^{-6} \pm 1.4 \times 10^{-7} \mu\text{M}^{-1} \text{ s}^{-1}$.

^e Saturation could not be reached, the data only allowed estimation of a minimal K_m value.

Table 3: Fast kinetic parameters for the ET processes of *Anabaena* WT and mutated Fld forms with Cyt c and WT FNR as determined by stopped-flow.

Fld form	Cyt c _{ox} + Fld _{hq}		FNR _{ox} + Fld _{hq}		FNR _{hq} + Fld _{ox}	
	k_{ap1} (s ⁻¹)	k_{ap2} (s ⁻¹)	k_{ap1} (s ⁻¹)	k_{ap2} (s ⁻¹)	k_{ap1} (s ⁻¹)	k_{ap2} (s ⁻¹)
WT	5.0	0.10	>600 ^{a,c}	- ^a	2.5 ^a	1.0 ^a
T12K	0.8	0.02	>600 ^c	-	13.5	1.3
T12V ^b	-	-	>600 ^c	45	1.0	0.5
E16K	6.3	0.20	83	18	2.2	0.4
E20K ^b	-	-	>600 ^c	245	15.5	1.3
E61K ^b	-	-	82	3.3	5.5	0.9
E67A	6.4	0.12	>340 ^c	4.0	8.0	1.5
D126K	7.8	0.21	>600 ^c	263	2.7	0.6
D144A	2.5	0.15	0.6	-	1.5	0.4
E16K/E61K	1.3	0.47	10	6.4	5.9	0.6
E16K/D126K	1.6	0.28	25	2.9	1.0	0.3
E16K/E20K/D126K	1.7	0.13	12	1.5	1.6	0.2
E16K/E61K/D126K/D150K	0.4	0.01	1.0	-	1.1	0.1
K2A/K3A	4.5	0.08	287	95	3.3	0.6
K2E/K3E	4.0	0.13	>470	127	2.7	0.5

^a Data were according to those published [25].

^b Data from [20].

^c Most of the reaction occurred within the instrumental dead time.

Table 4: Kinetic parameters for the reduction of *Anabaena* WT and mutated Fld_{ox} forms by PSI_{rd} studied by laser flash-photolysis. The reaction was followed at 580 nm.

Fld form	K_d (μM)	k_{et} (s^{-1})	k_2 ($\mu\text{M}^{-1}\text{s}^{-1}$)
WT	11.1	372	
T12K	4.31	39.5	
T12V ^a	10.0	130	
E16K	b	b	7
E20K ^a	b	b	3
E61K ^a	b	b	26
E67A	12.8	364	
D126K	b	b	9
D144A	b	b	12
E16K/E61K	b	b	19
E16K/D126K	b	b	11
E16K/E20K/D126K	b	b	0.4
E16K/E61K/D126K/D150K	9.1	848	
K2A/K3A	33.3	778	
K2E/K3E	b	b	10

^a Data from [20].

^b The dependence of k_{obs} on [Fld] was linear.

Figure Legends:

Figure 1. (A) UV-visible spectra obtained during photoreduction and redox titration of the E16K/E61K/D126K/D150K Fld mutant. (B) Nernst plots for the different oxidised/semiquinone Fld forms: WT (black circles), E67A (black stars), D144A (asterisks), E16K/E61K (black triangles), E16K/E61K/D126K/D150K (crossed circles), K2A/K3A (light grey squares), K2E/K3E (light grey triangles). (C) Nernst plots for the different semiquinone/hydroquinone Fld forms: WT (black circles), E61K (light grey rhombi), E67A (black stars), D144A (asterisks), E16K/E61K (black triangles), E16K/E61K/D126K/D150K (crossed circles), K2E/K3E (light grey triangles).

Figure 2. Spectroscopic characterization of WT FNR_{ox}:Fld_{ox} complexes: (A) Difference absorption spectra elicited by the binding to WT FNR_{ox} of WT (bold black line), T12K (bold dark grey line), D144A (grey circles), E16K/E61K (black circles), E16K/D126K (white circles), K2A/K3A (bold light grey line) Fld_{ox}, (B) Titration of WT FNR with WT (black circles), T12K (light grey stars), E16K (crossed circles), E67A (black stars), D126K (light grey circles), D144A (asterisks), E16K/E61K (black triangles), E16K/D126K (black squares), K2A/K3A (light grey squares), K2E/K3E (light grey triangles) Fld. Fittings for a 1:1 interaction are shown.

Figure 3. Time course for the anaerobic reactions between WT FNR and selected Fld mutants measured by stopped-flow methodology and follow at 600 nm. Kinetic traces for the reactions of WT FNR_{ox} with (A) WT (black circles), T12K (light grey stars), E67A (black stars), D144A (asterisks), K2A/K3A (light grey squares), K2E/K3E (light grey triangles) Fld_{hq}, (B) E16K (asterisks), E16K/E61K (black triangles), E16K/D126K (black squares), E16K/E20K/D126K (light grey stars), E16K/E61K/D126K/D150K (crossed circles) Fld_{hq}. Residuals for fittings of the K2E/K3E and E16K/E20K/D126K

Fld processes are shown at the bottom of the figures A and B, respectively. Kinetic traces for the reactions of WT FNR_{hq} with (C) WT (black circles), T12K (light grey stars), E67A (black stars), D144A (asterisks), K2A/K3A (light grey squares), K2E/K3E (light grey triangles) Fld_{ox}, (D) E16K (asterisks), D126K (light grey circles), E16K/E61K (black triangles), E16K/D126K (black squares), E16K/E20K/D126K (light grey stars), E16K/E61K/D126K/D150K (crossed circles) Fld_{ox}. Residuals for fittings of the D144A and E16K/E20K/D126K Fld processes are shown at the bottom of the Figures C and D, respectively.

Figure 4. Interaction and ET between WT and mutated Flds with WT PSI studied by laser flash-photolysis: Dependence of k_{obs} upon Fld concentration for reduction by PSI_{rd} of (A) WT (black circles), T12K (light grey stars), E67A (black stars), D144A (asterisks), K2A/K3A (light grey squares), K2E/K3E (light grey triangles) Fld_{ox} and, (B) WT (black circles), E16K (asterisks), D126K (light grey circles), E16K/E61K (black triangles), E16K/D126K (black squares), E16K/E20K/D126K (light grey stars), E16K/E61K/D126K/D150K (crossed circles) Flds_{ox}. Effect of MgCl₂ concentration on the k_{obs} for the reduction by PSI_{rd} of (C) WT (black circles), T12K (light grey stars), E67A (black stars), D144A (asterisks), K2A/K3A (light grey squares), K2E/K3E (light grey triangles) Flds_{ox} and (D) WT (black circles), E16K (asterisks), D126K (light grey circles), E16K/E61K (black triangles), E16K/D126K (black squares), E16K/E20K/D126K (light grey stars), E16K/E61K/D126K/D150K (crossed circles) Flds_{ox}.

Figure 5. (A) Detail of the FMN environment in the two monomers of the K2A/K3A Fld contained in their asymmetric units. CPK with C in different colours. Relevant H-bonds are shown in dotted lines. (B) Molecular surfaces with electrostatic potentials for

the X-ray structures of WT, E16K/E61K, E16K/E61K/D126K/D150K and K2A/K3A Flds. The FMN group is shown in sticks and CPK coloured with C in green.

Figure 6. (A) Magnitude and orientation of the dipole moments of K2A/K3A (violet arrow), K2E/K3E (orange arrow), E16K/D126K (yellow arrow), E16K/E61K/D126K/D150K (red arrow) and E16K/E61K (green arrow) Fld structures with regard to that of WT Fld (blue arrow). Two views rotated by 90° are shown. (B) Relative orientation of the molecular dipole moment of E16K/E61K/D126K/D150K Fld (red arrow) on the model for the docking interaction between FNR and Fld, dipoles for FNR and Fld are shown as black and blue arrows, respectively. (C) Model of the putative interaction of FNR and E16K/E61K/D126K/D150K Fld with a collinear orientation of their molecular dipole moments, but showing a relative disposition between the flavin rings not compatible with ET. Proteins are shown in blue cartoon for Fld and orange cartoon for FNR. The FMN and FAD groups are shown as sticks and CPK coloured with C in green and grey, respectively.

Figure 1

Figure 1

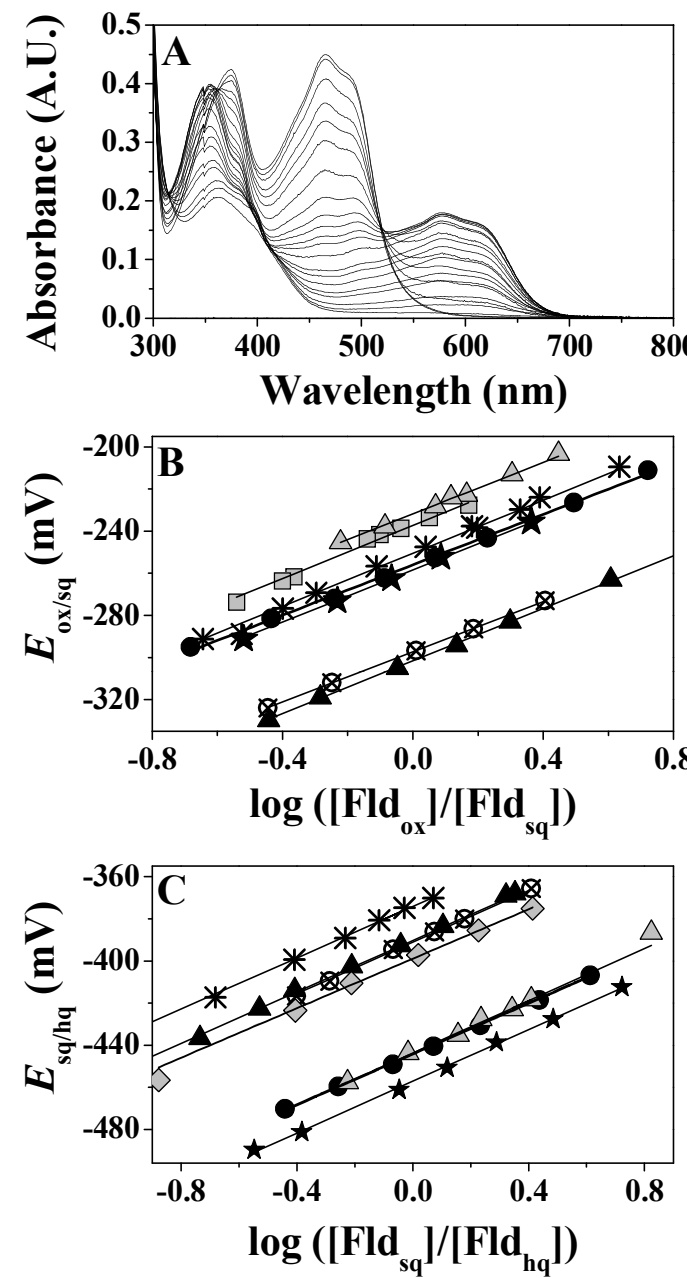


Figure 2

Figure 2

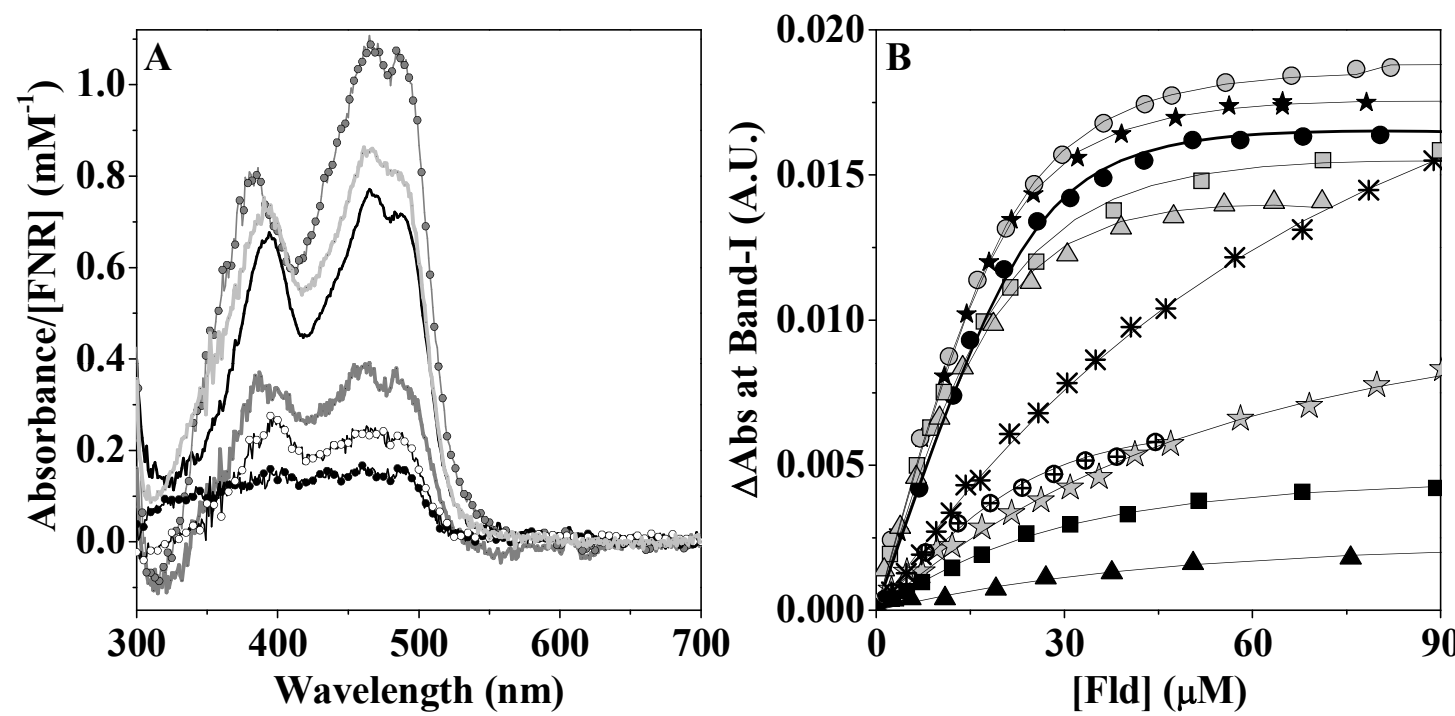


Figure 3

Figure 3

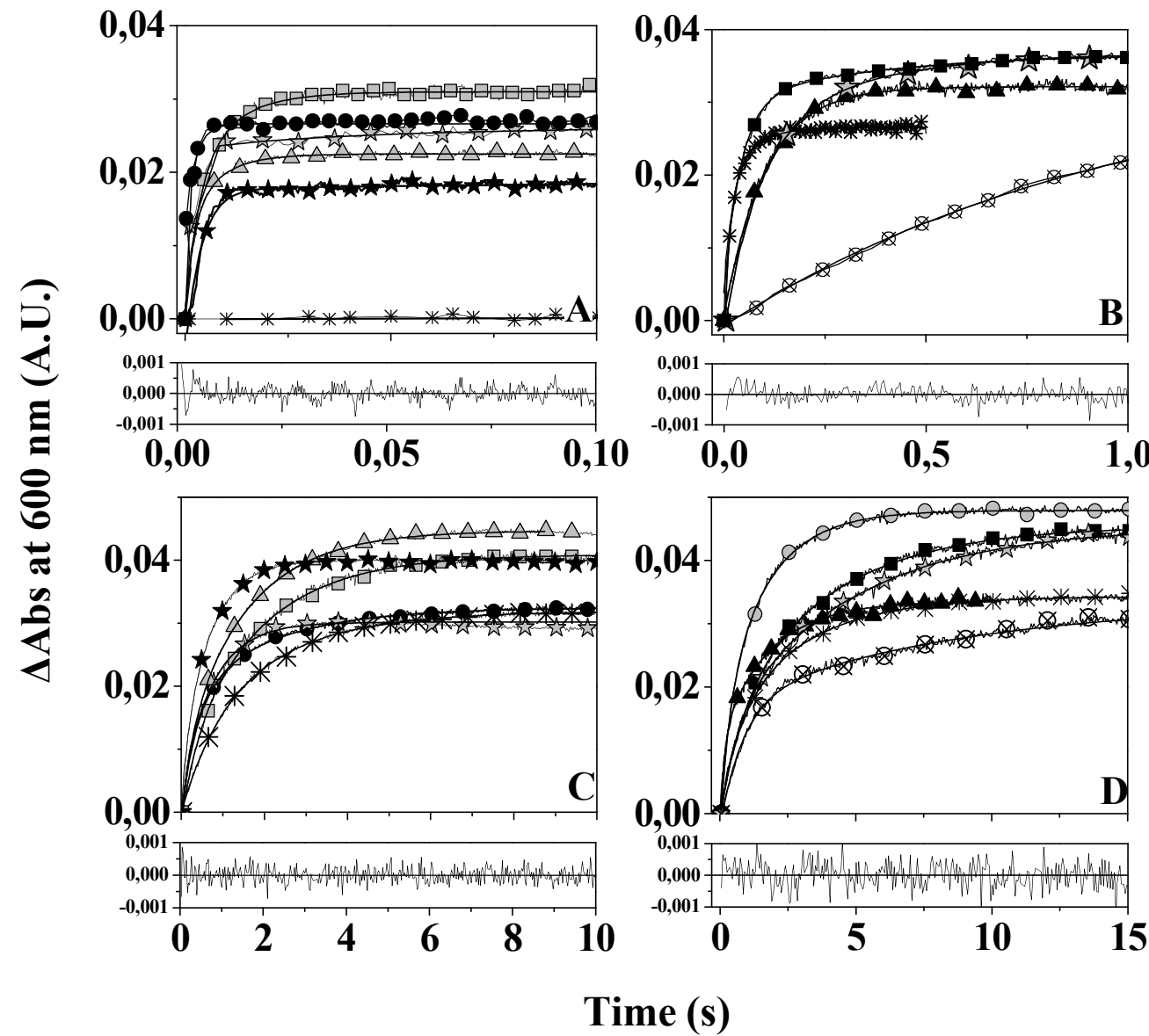


Figure 4

Figure 4

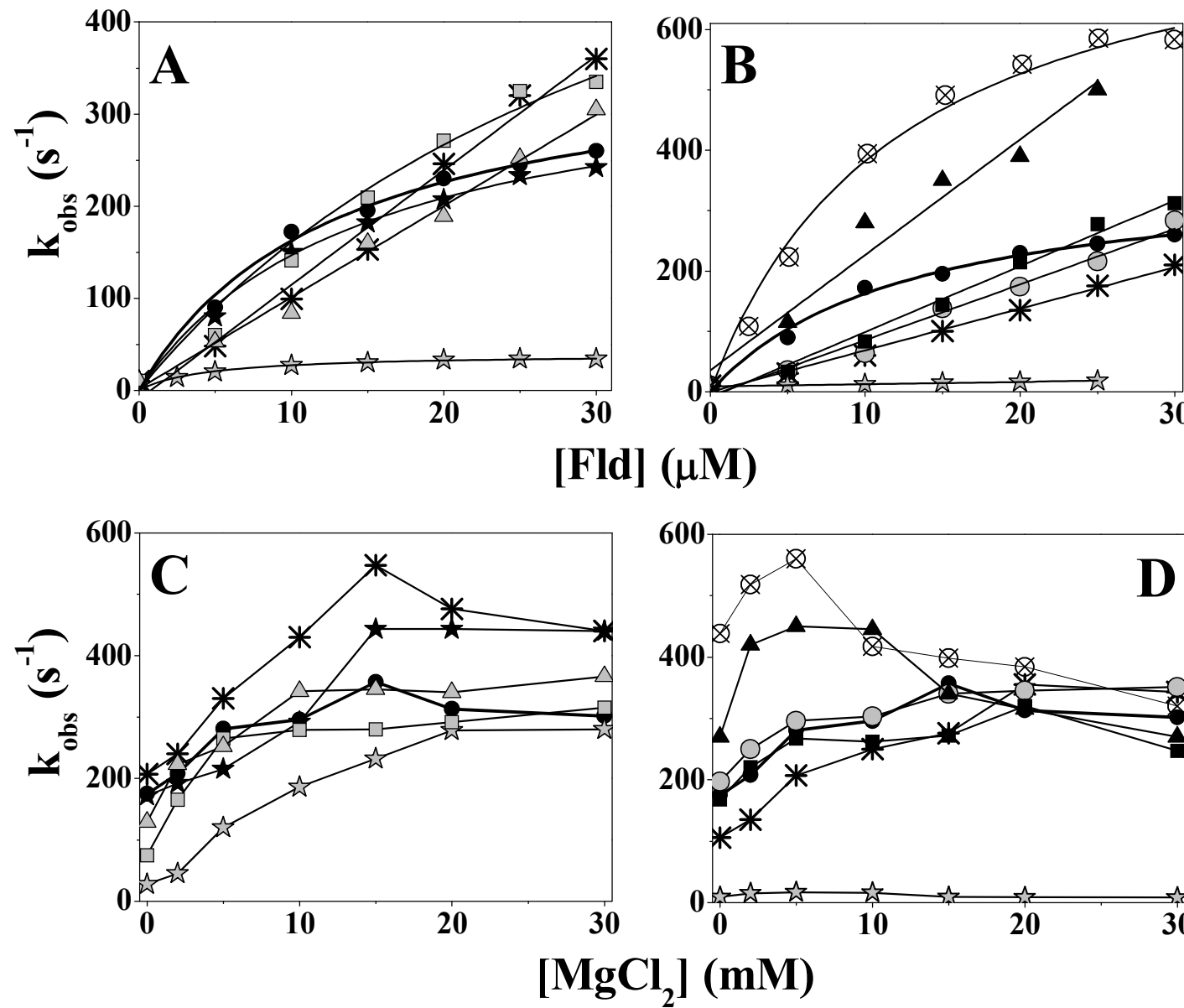


Figure 5

Figure 5

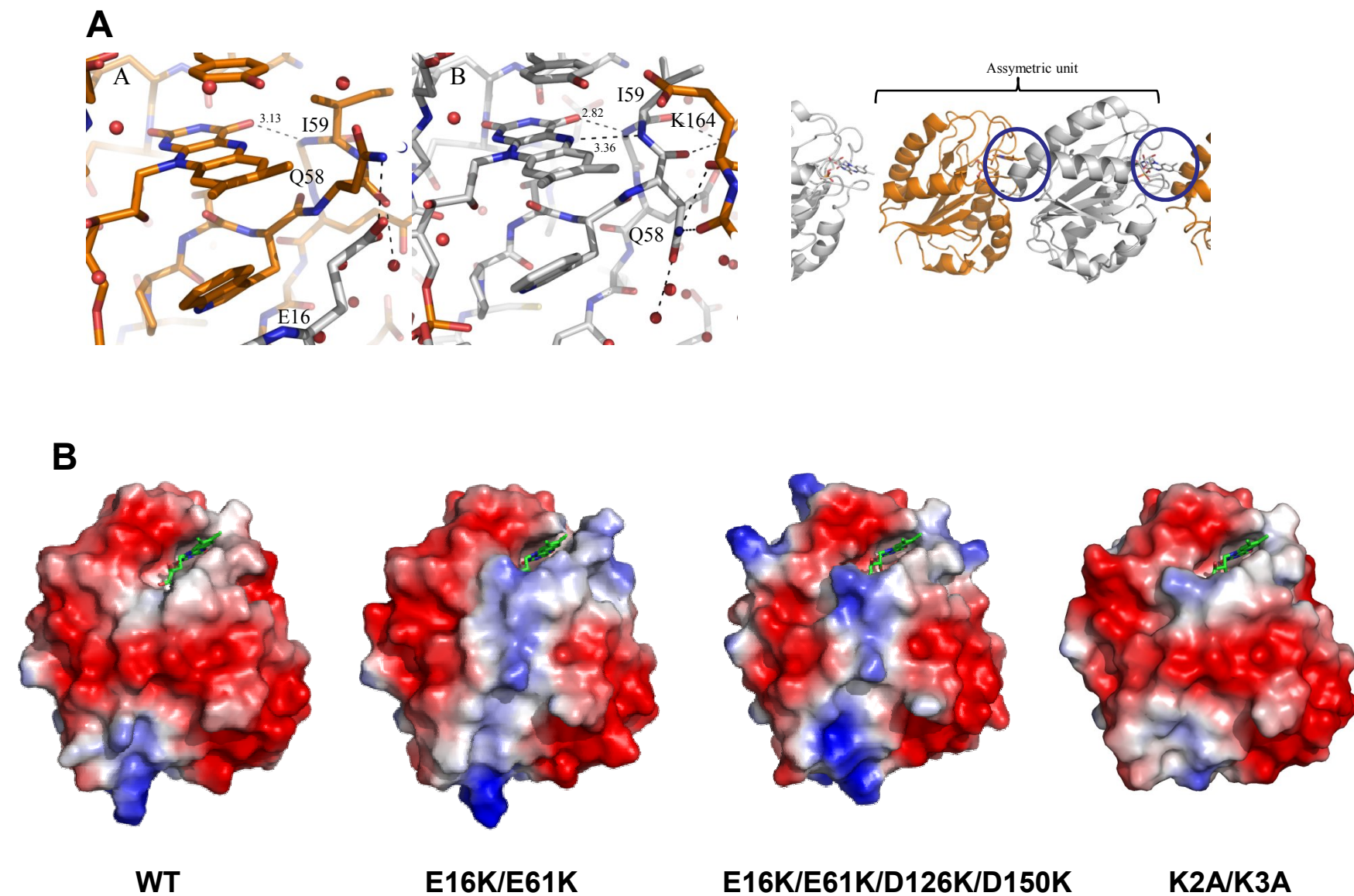
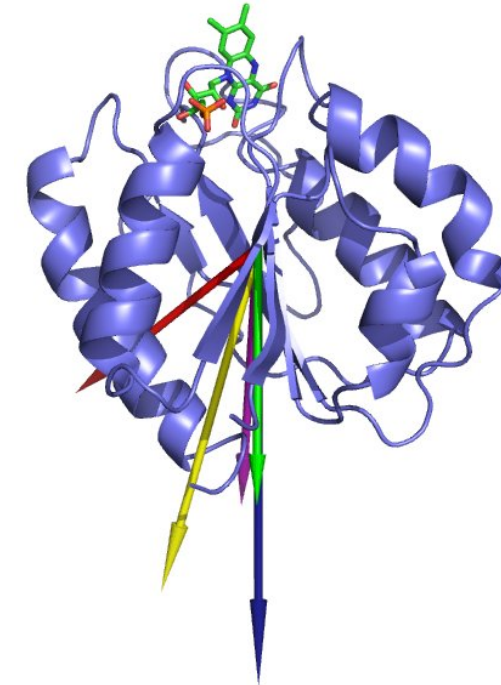
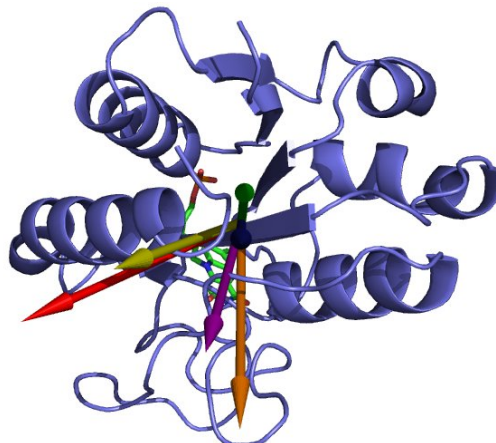


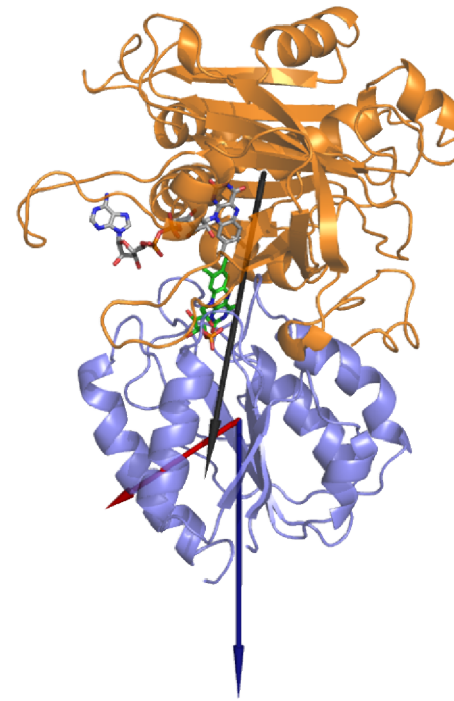
Figure 6

Figure 6

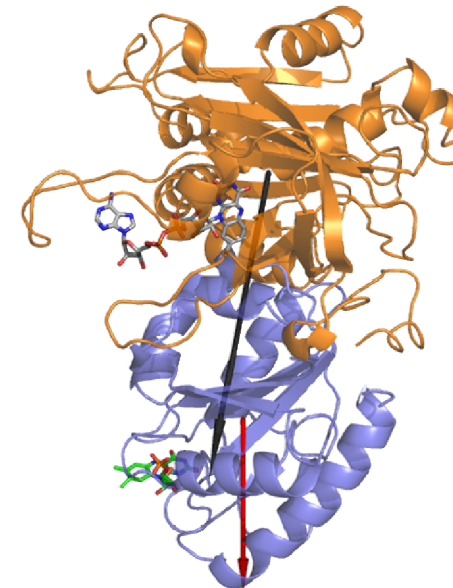
A



B



C



SUPPLEMENTARY MATERIAL

Materials and Methods

Synthetic oligonucleotides used for site directed mutagenesis, (5' to 3', modified bases in bold):

CAGACCATGGCAAAGG**C**AATTGGTTATTCTACGG for K3A,

CAGACCATGGCAG**CGG**CAATTGGTTATTCTACGG for K2A/K3A,

GAAACAGACCATGGCAG**AGG**AAATTGGTTATTCTACGG for K2E/K3E,

CTACGGTACTCAAA**AGG**TAAA**ACT**GAATCAGTAGCAG for T12K,

CTCAA**ACT**GGTAAA**ACT**AAGTCAGTAGCAGAAATCATTG for E16K,

CTGAATCAGTAGCGAAAATCATTGAGACGAGTTGG for E20K,

GGTAAA**ACT**AAGTCAGTAGCGAAAATCATTGAGACG for E16K/E20K,

CCTACTTGAATATTGGTAA**ACT**GCAAAGCGATTGGG for E61K,

GGTCAACTGATGGATATAAGTTAATGATTCCAAGGC for D126K and

GATGAAGATAATCAATCTAAGTTAACAGACGATCGC for D150K.

The oligonucleotides for the production of the E20K, E61K, E67A, D126K, D144A and D150K Fld mutants were previously designed [1, 2].

Spectral Analyses

The percentage of maximum semiquinone (sq) stabilised for each Fld was determined as the point of intersection of the resulting two lines of a plot of the absorbance at the wavelength of maximum absorbance of the semiquinone ($\text{Abs}^{\lambda_{\text{max}} \text{ sq}}$) *vs* the absorbance at the wavelength of maximum absorbance of the oxidised form ($\text{Abs}^{\lambda_{\text{max}} \text{ ox}}$) and the equation [3]:

$$\% \text{ sq}_{\text{stabilised}} = (\text{Abs}^{\lambda_{\text{max}} \text{ sq}}_{\text{experimental maximum}} / \text{Abs}^{\lambda_{\text{max}} \text{ sq}}_{\text{intersection}}) \times 100 \quad (1)$$

The extinction coefficient for the Fld_{sq} state at the wavelength of maximum absorbance of the semiquinone ($\epsilon^{\lambda_{\text{max}} \text{ sq}}$) was determined as:

$$\text{Abs}^{\lambda_{\text{max}} \text{ ox}}_{\text{initial}} / \epsilon^{\lambda_{\text{max}}}_{\text{ox}} = \text{Abs}^{\lambda_{\text{max}} \text{ sq}}_{\text{intersection}} / \epsilon^{\lambda_{\text{max}}}_{\text{sq}} \quad (2)$$

Midpoint Potentials Determination

The potential of the mediator dyes should be in the same range (± 60 mV) of that of the couple being analysed. At least two dyes were used in the same experiment as mediators for the two independent one-electron steps in the reduction of Fld. The following dyes were used (potential at pH 7 and 25 °C given in brackets); for the determination of $E_{\text{ox/sq}}$: Anthraquinone-2-sulfonic acid sodium salt (Fluka) (-225 mV) for WT, E67A, D126K, D144A, E16K/D126K, E16K/E20K/D126K, K2A/K3A, K2E/K3E Flds and Azocarmine G (Sigma) (-289 mV) for E61K, E16K/E61K, E16K/E61K/D126K/D150K Flds; for the determination of $E_{\text{sq/hq}}$: Methyl viologen dichloride (Sigma) (-440 mV) for WT, E67A, D126K, E16K/E20K/D126K, E16K/D126K, K2A/K3A, K2E/K3E Flds and Benzyl viologen dichloride (Sigma) (-359 mV) for E61K, D144A, E16K/E61K, E16K/E61K/D126K/D150K Flds. The protein solution was irradiated with light from a 250 W lamp for short periods of time. The potential of the solution after each illumination step was monitored by connecting the electrodes to a Fluke digital voltmeter via a buffer amplifier. The equilibrium of the system was considered established when the potential remained stable for 20 min. The UV/Vis spectrum was recorded in a Cary 100 Bio Varian spectrophotometer fitted with a thermostated holder and a magnetic stirrer. The optical spectrum was analysed at each step of the titration to calculate the concentration of every Fld redox species. The potential observed at each step was corrected according to the potential of the calomel electrode (-244.4 mV at 25 °C). Midpoint potentials for the oxido-reduction couples were calculated using the Nernst equation: $E = E_m + (0.059 / n) \log ([\text{ox}] / [\text{rd}])$ (3).

It is possible to independently determine the oxido-reduction midpoint potential for each of the two one-electron steps in Fld reduction, since only the oxidised and semiquinone forms were present during most of the first step and only semiquinone and hydroquinone were present during most of the second. Observed $E_{\text{ox/sq}}$ or $E_{\text{sq/hq}}$ values were plotted *vs* the logarithm of the ratio of concentration of the oxido-reduction couples ($[\text{ox}]/[\text{sq}]$ or $[\text{sq}]/[\text{hq}]$), respectively. Data points in the region of maximal semiquinone accumulation were not included in the analysis because, in this region, all three species could be present. At each step of the titration, the semiquinone concentration was calculated from the corresponding maximum absorbance ($\text{Abs}^{\lambda_{\text{max sq}}}$), and the concentration of the other species (ox or hq) was determined by subtraction of the semiquinone from the total concentration of Fld. The concentration ratios were calculated according to the following expressions:

$$[\text{ox}] / [\text{sq}] = (\text{Abs}^{\lambda_{\text{max sq}}} - \text{Abs}^{\lambda_{\text{max sq}}}_{100\% \text{ sq}}) / \text{Abs}^{\lambda_{\text{max sq}}} \quad (4)$$

$$[\text{sq}] / [\text{hq}] = \text{Abs}^{\lambda_{\text{max sq}}} / (\text{Abs}^{\lambda_{\text{max sq}}} - \text{Abs}^{\lambda_{\text{max sq}}}_{100\% \text{ sq}}) \quad (5)$$

Table SP1. Data collection and refinement statistics for Fld variants of *Anabaena* PCC 7119

	K2A/K3A Fld	E16K/E61K Fld	E16K/E61K/D126K/D150K Fld
Data collection statistics			
Space group	P2 ₁ 2 ₁ 2 ₁	P2 ₁ 2 ₁ 2 ₁	P2 ₁
Unit cell parameters (Å)	a = 58.67, b = 65.97, c = 75.64	a = 73.29, b = 74.82, c = 109.14	a = 37.60, b = 104.14, c = 37.80, β = 93.07
No. monomers/a.u.	2	4	2
Wavelength, Å	0.97918	1.5418	1.5418
Resolution, Å	43.84-1.94 (2.01-1.94)	47.21-2.39 (2.48-2.39)	37.76-2.31 (2.39-2.31)
No. of unique reflections	21900	24311	12191
Redundancy	6.0 (5.6)	7.8 (4.8)	1.7 (1.3)
Completeness, %	98.1 (95.4)	99.9 (99.2)	97.5 (89.99)
% reflections with I/σ > 2	97 (93.5)	87.4 (63.8)	97.7 (95)
R _{merge} ^a	0.057 (0.115)	0.078 (0.387)	0.036 (0.053)
Refinement statistics			
Resolution range, Å	30-1.94	22.72-2.39	18.57-2.31
Protein non-hydrogen atoms	2647	5304	2661
Metalic atoms	3	-	3
Ligand non-hydrogen atoms	62	136	62
Solvent non-hydrogen atoms	371	310	241
R _{work} (%)	15	19	18
R _{free} ^b (%)	20	25	24
rmsd bond lenght, Å	0.008	0.013	0.008
rmsd bond angles, °	1.126	1.496	1.216
Average B-factor, Å ²	15.48	21.48	10.71

Values in parentheses correspond to the highest resolution shell.

^a R_{sym} = $\sum |I - I_{av}| / \sum I$, where the summation is over symmetry equivalent reflections.^b R calculated for 7% of data excluded from the refinement.

Table SP2. UV/Vis spectral properties of WT and mutated Flds in the oxidised and semiquinone states. Data obtained in 50 mM Tris/HCl at pH 8.0 and 25 °C.

Fld form	Oxidised					Isosbestic points ox-sq (nm)	Semiquinone			
	λ_{\max} (nm)		ε_{\max} ($\text{mM}^{-1}\text{cm}^{-1}$)		$\varepsilon_I/\varepsilon_{II}$		λ_{\max} (nm)	ε_{\max} ($\text{mM}^{-1}\text{cm}^{-1}$)	% sq	
	I	II	I	II						
WT ^a	464	374	8.8	8.1	1.08	516	578	5.1	94	
T12K	464	374	9.0	8.25	1.09	517	577	4.0	93	
E16K	467	373	8.7	8.15	1.07	517	579	4.6	91	
E20K	465	374	9.0	8.0	1.11				94	
E61K	466	373	9.0	8.1	1.11	518	578	4.4	83	
E67A	465	374	9.1	8.2	1.11	515	577	5.1	96	
D126K	465	374	8.7	7.9	1.11	515	578	4.9	97	
D144A	463	374	9.6	8.5	1.04	515	578	4.6	86	
E16K/E61K	465	373	8.9	8.0	1.11	518	578	4.5	79	
E16K/D126K	464	374	8.9	8.0	1.11	516	577	5.0	94	
E16K/E20K/D126K	464	373	9.1	8.1	1.12	516	577	5.3	93	
E16K/E61K/D126K/D150K	466	374	8.9	8.0	1.11	519	578	4.5	80	
K2A/K3A	465	374	8.8	7.9	1.11	515	579	5.1	95	
K2E/K3E	465	374	8.7	7.9	1.10	515	578	5.0	95	
FMN	445	374	12.1	10.9	1.11					

^a Data were according to those published by [3, 4].

Table SP3: Dipole moments for WT and mutated Fld forms

Fld form	Deviation with regard to the WT				Dipole moment module (D)
	X (D)	Y (D)	Z (D)	Dipole moment (deg)	
WT	0.0	0.0	0.0	0.00	707
T12K	-8.2	-14	+4.0	0.82	627
E16K	+11	-21	-8.0	9.50	671
E20K	+19	-20	-4.3	10.91	687
E61K	-35	-15	+0.4	12.2	584
E67A	-15	-3.2	-6.4	6.25	676
D126K	-9.7	+5.1	+44	17.88	666
D144A	-5.5	+5.8	+2.3	3.16	715
E16K/E61K	-17	-42	-1.0	9.31	510
E16K/D126K	9.8	-19	35	15.13	615
E16K/E20K/D126K	28	-45	36	25.35	584
E16K/E61K/D126K/D150K	-12	-71	96	54.39	416
K2A/K3A	-35	-12	+30	15.77	557
K2E/K3E	-61	-15	+55	33.80	510

Figure Legends

Figure SP1. (A) Molecular surface with electrostatic potential of the putative Fd/Fld binding site of *Synechococcus elongatus* PSI (PDB code 1jb0) [5]. Surface presents a transparency to show the internal position of the F_A and F_B centres (represented as spheres) situated in the PsaC subunit of PSI. (B) Molecular surface with electrostatic potential of *Anabaena* FNR at the Fld docking site (PDB code 1que) [6]. The FAD

group is drawn in CPK coloured with carbons in orange. Key PSI and FNR positions for the interaction with the protein carrier are indicated. For PSI *Synechococcus* numbering is used. (C) Interaction surfaces of the Fld and FNR-like modules in the docking model for the *Anabaena* FNR:Fld interaction [7], the rat cytochrome P450 reductase (CYP450R) (PDB code 1amo) [8] and the nitric oxide synthase (NOS) (PDB code 1tl) structures [9]. FNR, Fld, CYP450R and NOS are shown as orange, blue, green and yellow cartoons, respectively. Fld residues analysed in this study at the interaction surface are shown as CPK sticks in Fld. Equivalent residues on CYP450R and NOS are similarly indicated. Conserved positions in NOS and CYP450R are similarly shown.

Figure SP2. Detail of the FMN environment in (A) the four monomers of the E16K/E61K Fld and (B) the two monomers of the E16K/E61K/D126K/D150K Fld. CPK with C in different colours. Relevant H-bonds are shown in dotted lines. In (A), residues belonging to a symmetrical molecule are coloured in grey.

Figure SP3. Environment of the isoalloxazine ring in Fld showing the position of residues D90, D144, E145 and D146.

Figure SP4. Surface electrostatic potential determined for the models of the different Fld variants.

REFERENCES

- [1] L.A. Campos, M.M. Garcia-Mira, R. Godoy-Ruiz, J.M. Sanchez-Ruiz and J. Sancho, *J Mol Biol* 344 (2004) 223-237.
- [2] J.A. Navarro, M. Hervás, C.G. Genzor, G. Cheddar, M.F. Fillat, M.A. de la Rosa, C. Gómez-Moreno, H. Cheng, B. Xia, Y.K. Chae and et al., *Arch Biochem Biophys* 321 (1995) 229-238.
- [3] I. Nogués, L.A. Campos, J. Sancho, C. Gómez-Moreno, S.G. Mayhew and M. Medina, *Biochemistry* 43 (2004) 15111-15121.
- [4] S. Frago, G. Goñi, B. Herguedas, J.R. Peregrina, A. Serrano, I. Pérez-Dorado, R. Molina, C. Gómez-Moreno, J.A. Hermoso, M. Martínez-Júlvez, S.G. Mayhew and M. Medina, *Arch Biochem Biophys* 467 (2007) 206-217.

- [5] P. Jordan, P. Fromme, H.T. Witt, O. Klukas, W. Saenger and N. Krauss, *Nature* 411 (2001) 909-917.
- [6] L. Serre, F.M. Vellieux, M. Medina, C. Gomez-Moreno, J.C. Fontecilla-Camps and M. Frey, *J Mol Biol* 263 (1996) 20-39.
- [7] M. Medina, R. Abagyan, C. Gomez-Moreno and J. Fernandez-Recio, *Proteins* 72 (2008) 848-862.
- [8] M. Wang, D.L. Roberts, R. Paschke, T.M. Shea, B.S. Masters and J.J. Kim, *Proc Natl Acad Sci U S A* 94 (1997) 8411-8416.
- [9] E.D. Garcin, C.M. Bruns, S.J. Lloyd, D.J. Hosfield, M. Tiso, R. Gachhui, D.J. Stuehr, J.A. Tainer and E.D. Getzoff, *J Biol Chem* 279 (2004) 37918-37927.

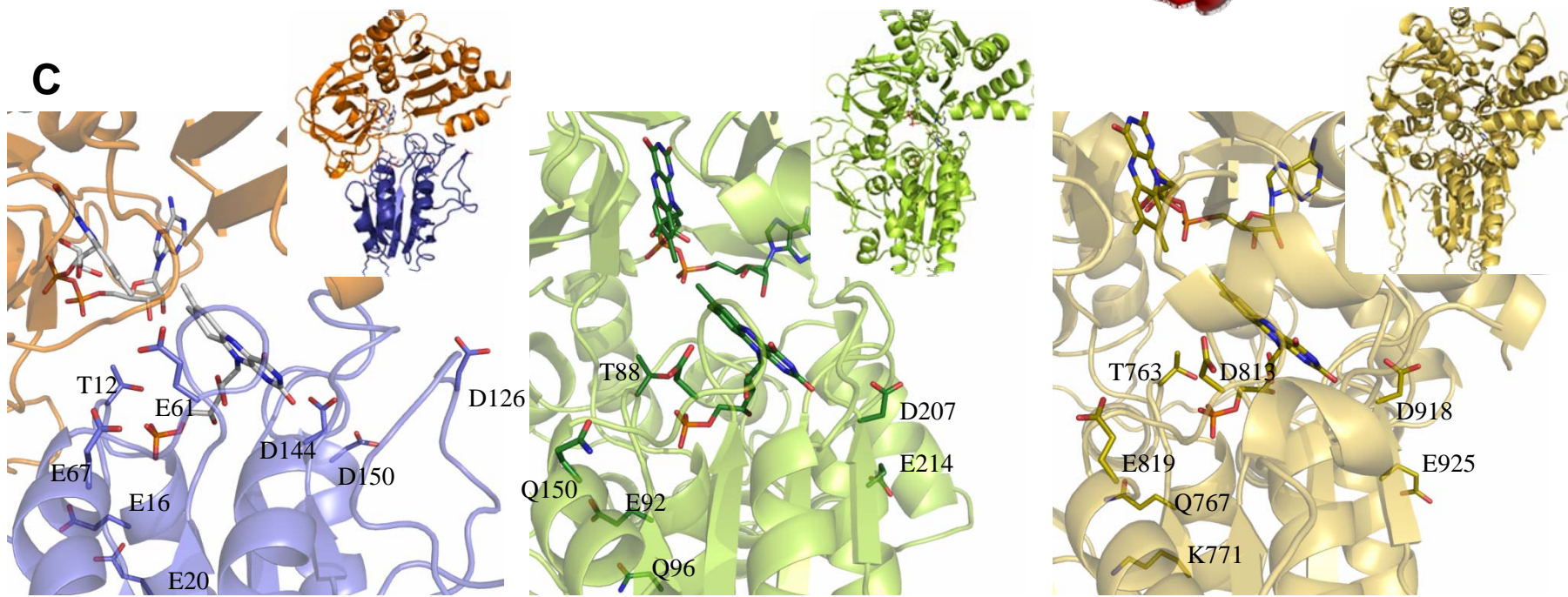
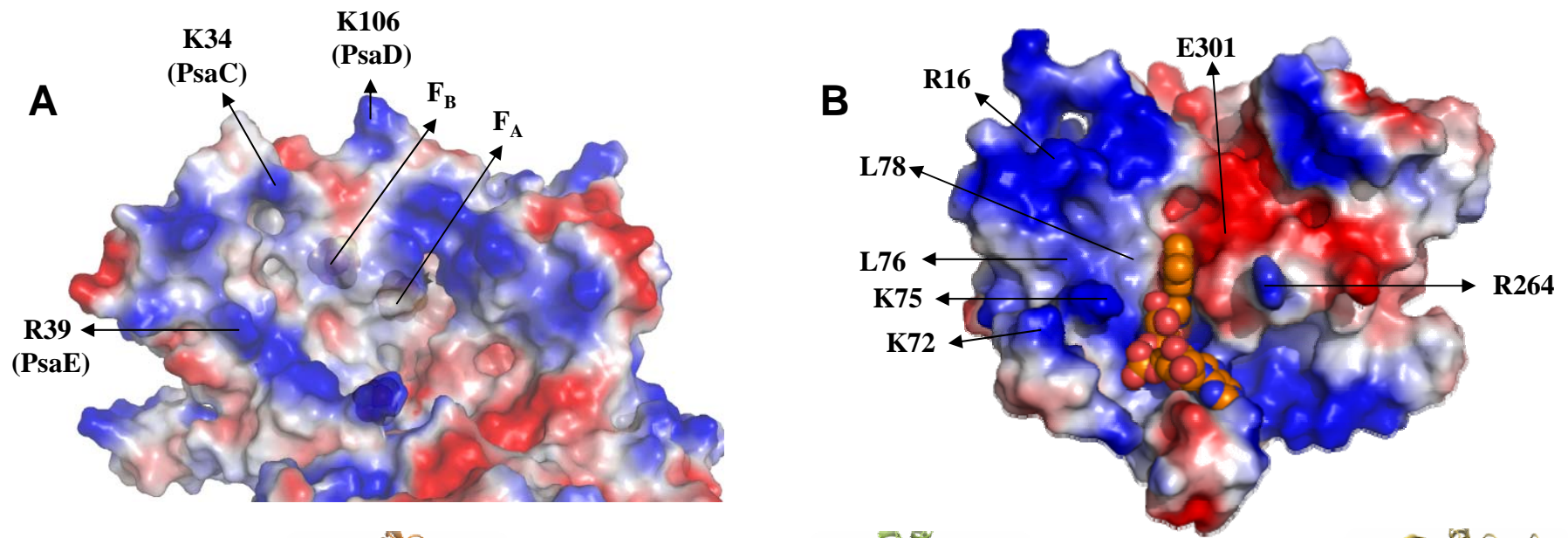
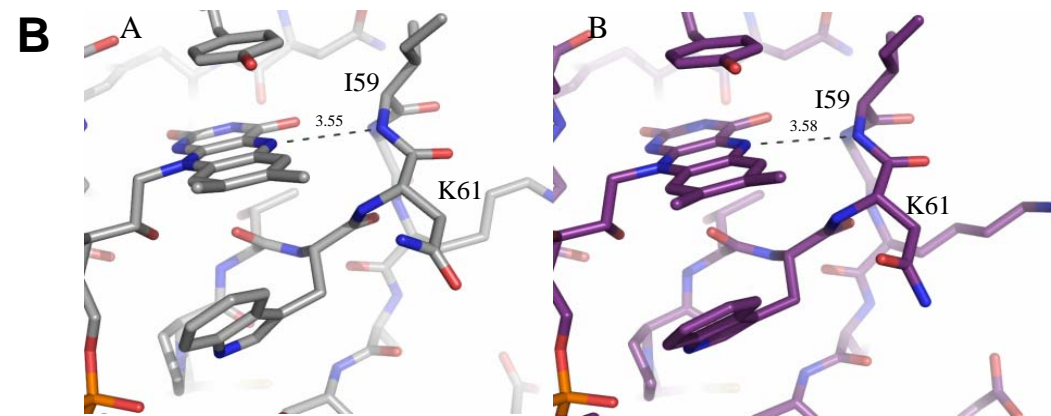
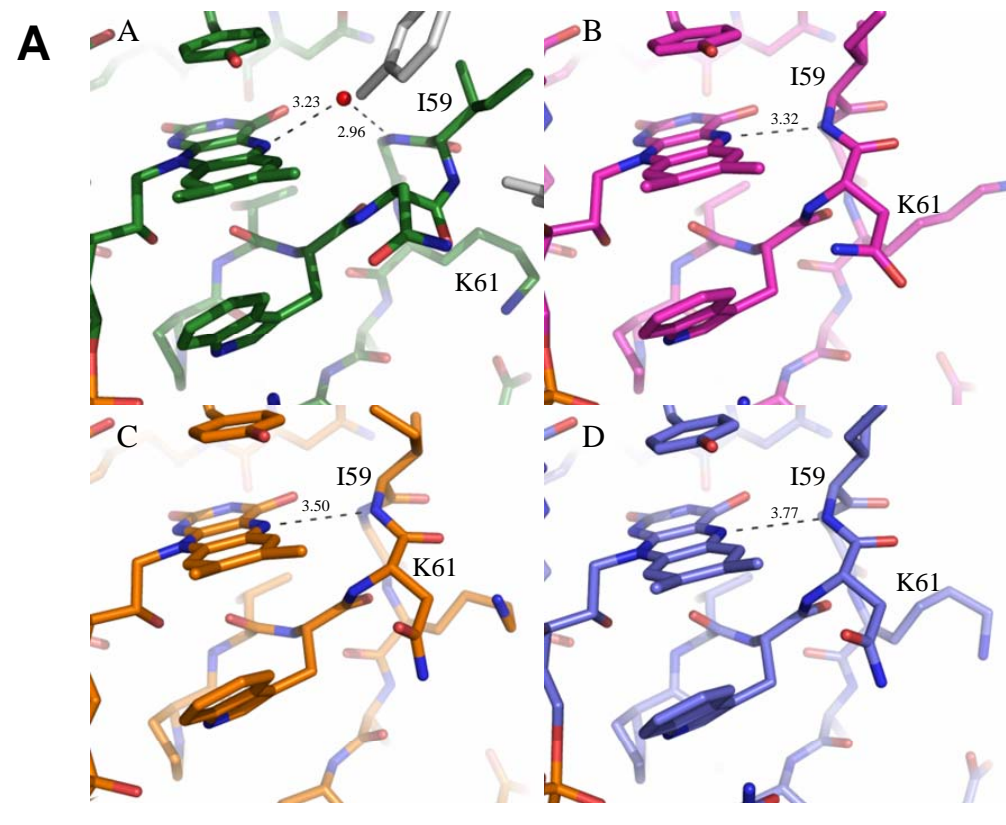


Figure SP1

Figure SP2



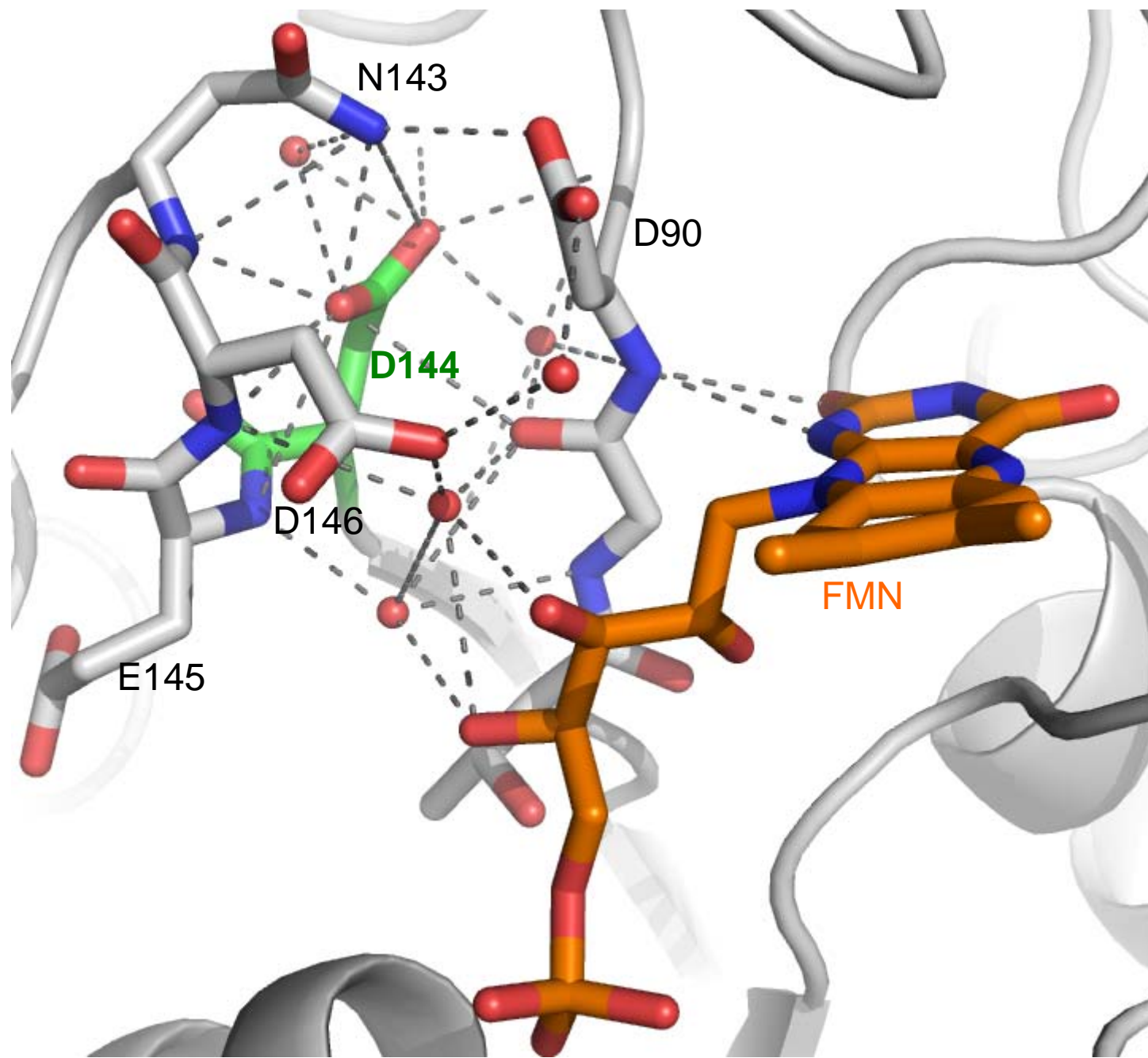
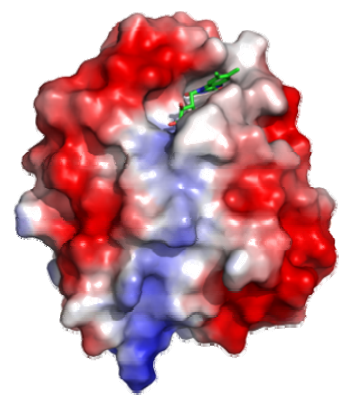
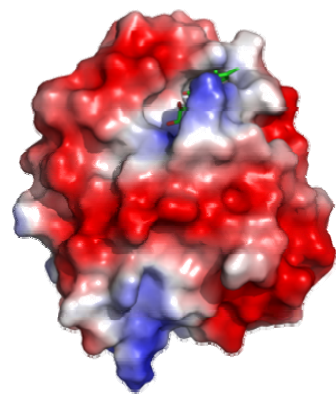


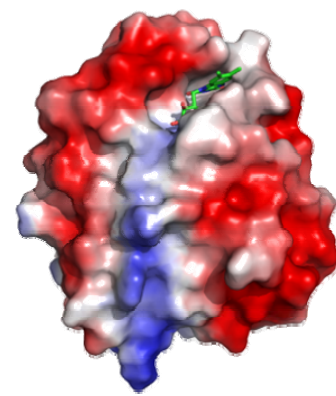
Figure SP3



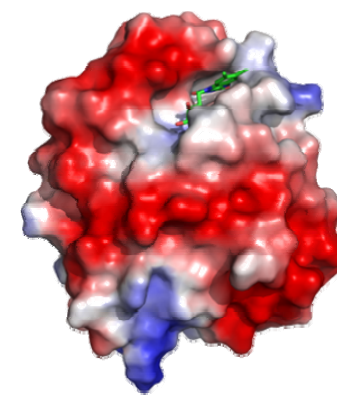
E16K



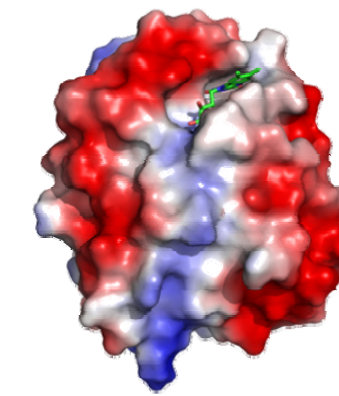
T12K



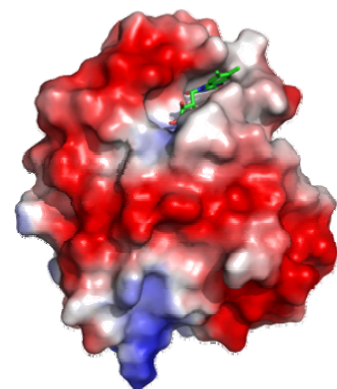
E20K



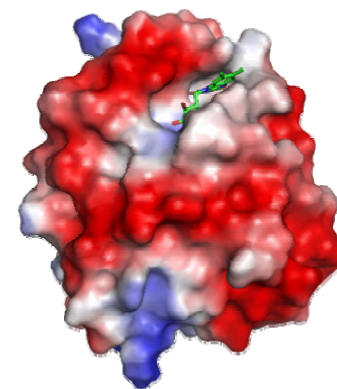
E61K



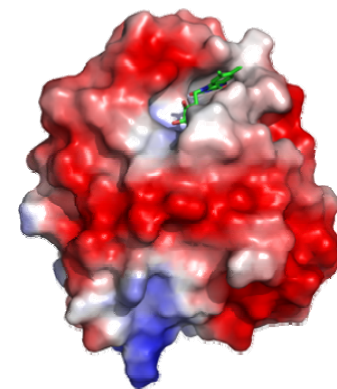
E16K/D126K



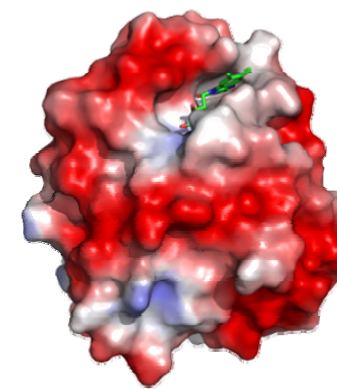
E67A



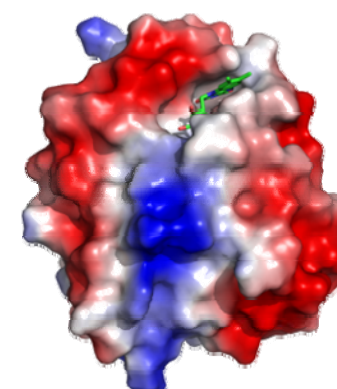
D126K



D144A



K2E/K3E



E16K/E20K/D126K

Figure SP4